diversity

MDPI

Article

Glyptothorax (Teleostei: Sisoridae) from the Middle East: An Integrated Molecular and Morphological Insight into Its Taxonomic Diversity

Golnaz Sayyadzadeh [1,2,†], Fatah Zarei [1,†] and Hamid Reza Esmaeili [1,*]

[1] Ichthyology and Molecular Systematics Research Laboratory, Department of Biology, School of Science, Shiraz University, Shiraz 7146713565, Iran
[2] Department of Biology, Faculty of Sciences, Lorestan University, Khorramabad 6815144316, Iran
* Correspondence: hresmaeili22@gmail.com or hresmaeili@shirazu.ac.ir
† These authors contributed equally to this work.

Abstract: The *Glyptothorax* species from the Middle East are taxonomically revised based on extensive geographic range and taxon sampling, tree topologies from mitochondrial COI and *Cyt* b and nuclear RAG2 markers (2532 bps), molecular species delimitation and genetic distance analyses of DNA sequences against morphometric and morphological characters. A majority-rule consensus based on conceptually different molecular species delimitation analyses combined with the Bayesian and maximum likelihood tree topologies considered all the name-bearing Iranian endemic clades of *Glyptothorax*, except for *G. pallens* (i.e., *G. alidaeii*, *G. galaxias*, *G. hosseinpanahii*, *G. shapuri* and *G. silviae*) as a single molecular entity. We also lent our years of experience to the morphology of Iranian *Glyptothorax* populations and tried to perceive consistent morphological differences, but without success. Therefore, based on this integrated molecular and morphological study, we treat *G. alidaeii*, *G. galaxias*, *G. hosseinpanahii and G. shapuri* as conspecific with *G. silviae*. Furthermore, our molecular and morphological results confirmed the first record of *G. cous* in Iranian waters. The species *G. armeniacus*, *G. cous*, *G. daemon*, *G. kurdistanicus*, *G. pallens*, *G. silviae* and *G. steindachneri* are considered as valid species.

Keywords: catfish; distribution; phylogenetic relationships; species delimitation; taxonomic diversity

Citation: Sayyadzadeh, G.; Zarei, F.; Esmaeili, H.R. *Glyptothorax* (Teleostei: Sisoridae) from the Middle East: An Integrated Molecular and Morphological Insight into Its Taxonomic Diversity. *Diversity* **2022**, *14*, 884. https://doi.org/10.3390/d14100884

Academic Editor: Simon Blanchet

Received: 15 September 2022
Accepted: 17 October 2022
Published: 20 October 2022

1. Introduction

Siluriformes is one of the most species-rich actinopterygian orders, with about 4131 valid species in 39 families, including the family Sisoridae [1]. Members of the sisorid catfish genus *Glyptothorax* Blyth, 1860 (Siluriformes: Sisoridae) are typically inhabited in fast-flowing hill streams or faster-flowing reaches of larger rivers from Asia (in the Tigris and Euphrates River drainages of Türkiye, Syria, Iraq and Iran), eastward to the Yangtze River drainage and southward to South-East Asia [2,3]. It is the most species-rich and widely distributed genus in the family, with new species being discovered regularly [1]. Until 2021, no data were published on the taxonomic revision of this genus in the Middle East. Recently, Freyhof et al. [4] and Mousavi-Sabet et al. [5] revised the *Glyptothorax* of the Euphrates, Tigris and the Persis River tributaries (i.e., the Persian Gulf basin) based on the morphological and mtDNA COI barcode region and described six new species.

Here, based on our available data since 2009, we present morphological and molecular (mitochondrial COI and *Cyt* b and nuclear RAG2) data to (i) provide the first multilocus phylogeny of the genus *Glyptothorax* in the Middle East, (ii) investigate the validity of newly described species from Iran and also species-level diversity within the genus in the area and (iii) update the distributional ranges for the species and lineages based on new samplings and DNA sequence data. To recognize the number of valid species within the genus *Glyptothorax* in the region, we identify distinct lineages based on tree topologies

(mitochondrial COI sequence data) as 'molecular species'. We then seek morphological differences to differentiate the 'molecular species' hypothesized by the tree topology and molecular species delimitations. This publication was postponed by more than a decade as we tried multiple times to find morphological differences between the Iranian molecular clades recognized in this genus. Results should provide a primary understanding of the genus taxonomic diversity and distribution in the region, which are relevant for future taxonomic efforts and formulating conservation strategies and management proposals.

2. Materials and Methods

2.1. Sampling and Morphological Measurements

New samples of *Glyptothorax* were collected from 21 Iranian localities in the tributaries of the Persian Gulf basin (Figure 1; Table 1). Specimens were collected using an electrofishing device. Clove oil solution (1%) was used as an anesthetic.

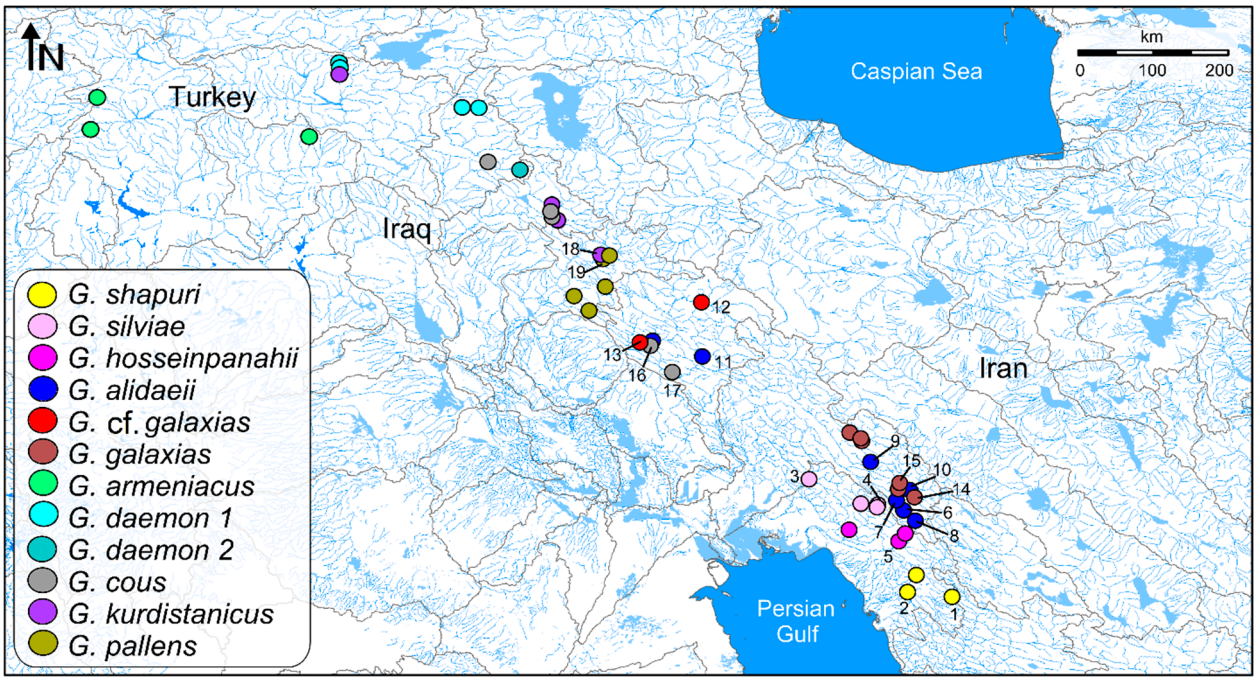

Figure 1. Records of *Glyptothorax* spp. from the Middle East used in this study. The location codes (new localities from Iran) correspond to those in Table 1. Un-numbered localities refer to those from Freyhof et al. [4] and Mousavi-Sabet et al. [5]. The map was originally designed in DIVA-GIS 7.5 (https://www.diva-gis.org/) (accessed on 28 February 2022).

Morphometric measurements were made with a dial calliper and recorded to 0.1 mm. All measurements were made point to point, never by projections. Subunits of the head are presented as proportions of head length (HL). Head length and measurements of body parts are given as proportions of standard length (SL). Methods for counts and measurements follow Ng and Dodson [6], except for caudal fin length which was measured as the length of the largest ray of the upper lobe.

For molecular analysis, the right pectoral fin of some specimens was clipped and fixed in 96% ethanol, while the voucher specimens were kept in 10% formaldehyde and subsequently stored in 70% ethanol. These specimens are deposited in the Zoological Museum of Shiraz University, Collection of Biology Department (ZM-CBSU). Additional *Glyptothorax* specimens (*G. daemon* and *G. armeniacus*) were also included from Türkiye (Table 1).

Abbreviations used. SL, standard length; HL, lateral head length.

Collection codes. BMNH, Natural History Museum, London; CMNFI, Canadian Museum of Nature; ZFMK, Zoologisches Forschungsmuseum Alexander Koenig; ZM-CBSU, Zoological Museum of Shiraz University, Collection of Biology Department, Shiraz.

Table 1. List of novel and previously studied *Glyptotorax* spp. specimens from the Middle East used in this study. Sequences used for the combined analysis (COI + *Cyt* b + RAG2) are marked with Greek numbers (I–XXIII). Source: A, Mousavi-Sabet et al. [5]; B, Freyhof et al. [4]; C, this study (GenBank numbers are given in Table S3); † a possible hybrid population (see Freyhof et al. [4]; ‡ new locality numbers refer to the new sampling sites from Iran, as shown in Figure 1.

Species	Source	COI	*Cyt* b	RAG2	Latitude	Longitude	Locality Code ‡	Locality
G. shapuri	A	MZ959031			29.762	51.551		Iran: Fars prov., Shapur River at Eslamabad
G. shapuri	A	MZ959032			29.762	51.551		Iran: Fars prov., Shapur River at Eslamabad
G. shapuri	C		GY292 [I]		29.394	52.161	1	Iran: Helleh, Kohmareh Sorkhi stream
G. shapuri	C	G396 [I, II]	P396 [II]	G396R [II]	29.394	52.161	1	Iran: Helleh, Kohmareh Sorkhi stream
G. shapuri	C	G970F			29.467	51.395	2	Iran: Konar Takhteh, Helleh, Dalaki River
G. shapuri	C	G971F			29.467	51.395	2	Iran: Konar Takhteh, Helleh, Dalaki River
G. shapuri	C	G333 [III]	GY333 [III]		29.394	52.161	1	Iran: Helleh, Kohmareh Sorkhi stream
G. shapuri	C	G401 [IV]	G401 [IV]	G401R [IV]	29.394	52.161	1	Iran: Helleh, Kohmareh Sorkhi stream
G. silviae	C	G395			31.376	49.730	3	Iran: Khuzestan, Ab-e Aala River, Baghmalek
G. silviae	C	G410 [V]			31.376	49.730	3	Iran: Khuzestan, Ab-e Aala River, Baghmalek
G. silviae	C		GY330 [V]		30.949	50.904	4	Iran: Kohgiluyeh and Boyer-Ahmad prov., Maroun River at Garab-e-Lodab
G. silviae	C	G589 [VI]	GY295 [VI]	G589R [VI]	31.376	49.730	3	Iran: Khuzestan, Ab-e Aala River, Baghmalek
G. silviae	C	G411 [VII]	G411 [VII]	G411R [VII]	31.376	49.730	3	Iran: Khuzestan, Ab-e Aala River, Baghmalek
G. silviae	A	MZ959028			30.946	50.904		Iran: Kohgiluyeh-va-Boyer Ahmad prov., Maroun River at Garab-e-Lodab
G. silviae	A	MZ959029			30.946	50.904		Iran: Kohgiluyeh-va-Boyer Ahmad prov., Maroun River at Garab-e-Lodab
G. silviae	A	MZ959030			30.959	50.615		Iran: Kohgiluyeh-va-Boyer Ahmad prov., Maroun River at Qale-Gol
G. hossein-panahii	C	G597 [VIII]	GY294 [VIII]	G597R [VIII]	30.328	51.251	5	Iran: Fars prov., Zohreh, Fahlian River
G. hossein-panahii	C	G598 [IX]	GY332 [IX]	G598R [IX]	30.328	51.251	5	Iran: Fars prov., Zohreh, Fahlian River

Table 1. *Cont.*

Species	Source	COI	*Cyt* b	RAG2	Latitude	Longitude	Locality Code ‡	Locality
G. hossein-panahii	A	MZ959033			30.461	51.353		Iran: Kohgiluyeh-va-Boyer Ahmad prov., Zohreh River at Tange-Shiv
G. hossein-panahii	A	MZ959034			30.530	50.416		Iran: Khuzestan prov., Zohreh River at Kheirabad
G. hossein-panahii	A	MZ959035			30.461	51.353		Iran: Kohgiluyeh-va-Boyer Ahmad prov., Zohreh River at Tange-Shiv
G. alidaeii	C	ZM-CBSU Ex58F4			30.852	51.342	6	Iran: Kohgiluyeh and Boyer-Ahmad prov., Khersaan River at Betari
G. alidaeii	C	G606			31.040	51.218	7	Iran: Kohgiluyeh and Boyer-Ahmad prov., Khersaan River
G. alidaeii	C	ZM-CBSU Ex58F3			30.852	51.342	6	Iran: Kohgiluyeh and Boyer-Ahmad prov., Khersaan River at Betari
G. alidaeii	C	G414 [X, XI, XII]	G414 [X]	G414R [X]	30.676	51.532	8	Iran: Kohgiluyeh and Boyer-Ahmad prov., Beshar River at Aliabade-e Satrol
G. alidaeii	C		GY326 [XI]		31.670	50.769	9	Iran: Chaharmahal and Bakhtiari prov., Armand River
G. alidaeii	C		GY329 [XII]		31.184	51.450	10	Iran: Isfahan prov., Bibi Seyedan
G. alidaeii	B	MW770731			30.852	51.342		Iran: Beshar at Doruhan
G. alidaeii	B	MW770718			30.852	51.342		Iran: Beshar at Doruhan
G. alidaeii	A	MZ959036			33.688	47.064		Iran: Lorestan prov., Seimare River at Zirkhaki
G. alidaeii	A	MZ959037			33.688	47.064		Iran: Lorestan prov., Seimare River at Zirkhaki
G. alidaeii	C	G728F [XIII]	G728b [XIII]	G835R [XIII]	33.458	47.930	11	Iran: Lorestan prov., Kashkan River, Ghalebi-e-Sofla village Betwwen Khoramabad and Mamulan Lorestan
G. alidaeii	C	G726F			33.458	47.930	11	Iran: Lorestan prov., Kashkan River, Ghalebi-e-Sofla village Betwwen Khoramabad and Mamulan Lorestan
G. alidaeii	C	G729F			33.458	47.930	11	Iran: Lorestan prov., Kashkan River, Ghalebi-e-Sofla village Betwwen Khoramabad and Mamulan Lorestan

Table 1. *Cont.*

Species	Source	COI	*Cyt* b	RAG2	Latitude	Longitude	Locality Code ‡	Locality
G. alidaeii	C	G727F			33.458	47.930	11	Iran: Lorestan prov., Kashkan River, Ghalebi-e-Sofla village Betwwen Khoramabad and Mamulan Lorestan
G. cf. *galaxias*	C	G323 [XIV]	GY323 [XIV]	G323R [XIV]	34.371	47.912	12	Iran: Hamadan prov., Gamasiab River at Do Ab
G. cf. *galaxias*	C	G558 [XV, XVI]	G558b [XV]	G558R [XV]	33.694	46.883	13	Iran: Ilam prov., Chardaval River
G. cf. *galaxias*	C		G557b [XVI]	G557R [XVI]	33.694	46.883	13	Iran: Ilam prov., Chardaval River
G. cf. *galaxias*	C	G296 [XVII]	GY296 [XVII]	G296R [XVII]	34.371	47.912	12	Iran: Hamadan prov., Gamasiab River at Do Ab
G. galaxias	A	MZ959025 [XVIII]			32.029	50.627		Iran: Chaharmahal-va-Bakhtiari prov., stream Beheshtabad at Beheshtabad
G. galaxias	C		GY327 [XVIII]		31.078	51.518	14	Iran: Isfahan prov., Khak Daneh
G. galaxias	A	MZ959026			32.165	50.423		Iran: Chaharmahal-va-Bakhtiari prov., stream Afsarabad at Afsarabad
G. galaxias	A	MZ959027 [XIX]			31.280	51.266		Iran: Chaharmahal-va-Bakhtiari prov., stream Mal-e-Khalife at Mal-e-Khalife
G. galaxias	C		GY325 [XIX]	G331R [XIX]	31.186	51.256	15	Iran: Kohgiluyeh and Boyer-Ahmad prov., Kata
G. galaxias	B	MW770721			32.034	50.633		Iran: Behesht Abad River north of Ardal, 75 km south-west of Shahr-e-kord
G. armeni-acus	B	MW770712			37.173	41.270		Türkiye: Tunceli prov., stream Pülümür at Pülümür
G. armeni-acus	B	MW724503			37.292	37.573		Türkiye: Gaziantep prov., stream Merzimen 3 km south of Yavuzeli
G. armeni-acus	C	G834						Türkiye: Pueluemuer
G. armeni-acus	ZFMK	ZFMK FSJF-2634			37.837	37.685		Türkiye: upper River Göksu 5 km northeast of Gölbaşı
G. armeni-acus	ZFMK	ZFMK FSJF-2634-2			37.837	37.685		Türkiye: upper River Göksu 5 km northeast of Gölbaşı
G. armeni-acus	C	G369						Türkiye: Pueluemuer

Table 1. *Cont.*

Species	Source	COI	*Cyt* b	RAG2	Latitude	Longitude	Locality Code ‡	Locality
G. armeniacus	B	MW770726			37.837	37.685		Türkiye: upper River Göksu, 5 km northeast of Gölbaşı
G. armeniacus	B	MW770714			37.837	37.685		Türkiye: upper River Göksu, 5 km northeast of Gölbaşı
G. armeniacus	B	MW770723			37.837	37.685		Türkiye: Tunceli prov., stream Pülümür at Pülümür
G. daemon 1	C	G931F						Türkiye: Greater Zab
G. daemon 1	B	MW724515			37.672	43.863		Türkiye: Hakkari prov., stream Eziki 6 km northeast Konak
G. daemon 1	B	MW724520			38.355	41.781		Türkiye: Bitlis prov., stream Çıratan 3 km southwest of Üçadım
G. daemon 1	B	MW724519			38.355	41.781		Türkiye: Bitlis prov., stream Çıratan 3 km southwest of Üçadım
G. daemon 1	B	MW724518			38.355	41.781		Türkiye: Bitlis prov., stream Çıratan 3 km southwest of Üçadım
G. daemon 1	B	MW724514			37.672	43.863		Türkiye: Hakkari prov., stream Eziki 6 km northeast Konak
G. daemon 1	B	MW770713			38.385	41.782		Türkiye: stream Çıratan about 5 km east of Gümüşkanat
G. daemon 1	B	MW770729			38.385	41.782		Türkiye: stream Çıratan about 5 km east of Gümüşkanat
G. daemon 1	C	G559						Türkiye Yukeskora Hakkari prov Yukeskora
G. daemon 1	B	MW724516			37.672	43.863		Türkiye: Hakkari prov., stream Eziki 6 km northeast Konak
G. daemon 1	B	MW770722			37.666	44.139		Türkiye: Hakkari prov., stream Dilektaşı 16 km northeast Yüksekova
G. daemon 2 †	B	MW724512			37.666	44.139		Türkiye: Hakkari prov., stream Dilektaşı 16 km northeast Yüksekova
G. daemon 2 †	B	MW724513			37.666	44.139		Türkiye: Hakkari prov., stream Dilektaşı 16 km northeast Yüksekova
G. daemon 2 †	B	MW724517			37.666	44.139		Türkiye: Hakkari prov., stream Dilektaşı 16 km northeast Yüksekova

Table 1. *Cont.*

Species	Source	COI	*Cyt* b	RAG2	Latitude	Longitude	Locality Code ‡	Locality
G. daemon 2 †	B	MW770730			36.611	44.838		Iraq: stream Choman at Qubay Galala
G. daemon 2 †	B	MW770732			36.611	44.838		Iraq: stream Choman at Qubay Galala
G. daemon 2 †	B	MW770733			36.611	44.838		Iraq: stream Choman at Qubay Galala
G. daemon 2 †	B	MW770724			36.611	44.838		Iraq: stream Choman at Qubay Galala
G. daemon 2 †	B	MW770725			36.611	44.838		Iraq: stream Choman at Qubay Galala
G. cous	B	MW724510			35.915	45.368		Iraq: Qal'ah Chwalan River at Bardbard
G. cous	B	MW724509			35.915	45.368		Iraq: Qal'ah Chwalan River at Bardbard
G. cous	B	MW724504			35.915	45.368		Iraq: Qal'ah Chwalan River at Bardbard
G. cous	B	MW724511			35.915	45.368		Iraq: Qal'ah Chwalan River at Bardbard
G. cous	B	MW724508			35.915	45.368		Iraq: Qal'ah Chwalan River at Bardbard
G. cous	B	MW724507			35.915	45.368		Iraq: Qal'ah Chwalan River at Bardbard
G. cous	B	MW770716			35.751	45.479		Iraq: Aw-e Shiler River at Khewata
G. cous	B	MW770715			35.751	45.479		Iraq: Aw-e Shiler River at Khewata
G. cous	B	MW770719			35.751	45.479		Iraq: Aw-e Shiler River at Khewata
G. cous	B	MW770727			36.748	44.300		Iraq: Great Zab about 2 km upriver of confluence with Rawanduz River
G. cous	B	MW724505			35.915	45.368		Iraq: Qal'ah Chwalan River at Bardbard
G. cous	B	MW724506			35.915	45.368		Iraq: Qal'ah Chwalan River at Bardbard
G. cous	C	G324 [XX]	GY324 [XX]	G324R [XX]	33.680	47.055	16	Iran: Ilam prov., Seimare River
G. cous	C	G368 [XXI]	G368 [XXI]	G368R [XXI]	33.183	47.417	17	Iran: Ilam prov., Seimare River
G. kurdistanicus	C	G510 [XXII]	G510b [XXII]	G510R [XXII]	35.118	46.257	18	Iran: Kermanshah prov., Sirwan River
G. kurdistanicus	B	MW724521			35.915	45.368		Iraq: Qal'ah Chwalan River at Bardbard
G. kurdistanicus	B	MW770728			35.751	45.480		Iraq: Aw-e Shiler at Khewata
G. kurdistanicus	B	MW770720			35.751	45.480		Iraq: Aw-e Shiler at Khewata

Table 1. *Cont.*

Species	Source	COI	*Cyt* b	RAG2	Latitude	Longitude	Locality Code ‡	Locality
G. kurdistanicus	B	MW770717			35.751	45.480		Iraq: Aw-e Shiler at Khewata
G. kurdistanicus	B	MW724523			38.355	41.781		Türkiye: Bitlis prov., stream Çıratan 3 km southwest of Üçadım
G. kurdistanicus	B	MW724522			38.355	41.781		Türkiye: Bitlis prov., stream Çıratan 3 km southwest of Üçadım
G. kurdistanicus	B	MW724524			38.355	41.781		Türkiye: Bitlis prov., stream Çıratan 3 km southwest of Üçadım
G. pallens	A	MZ959042			34.481	45.756		Iran: Kermanshah prov., stream Alvand near Qasr-e-Shirin
G. pallens	A	MZ959038			34.645	46.286		Iran: Kermanshah prov., stream Zemkan 3 km north of Zamkan-e Olya
G. pallens	A	MZ959041			34.228	46.004		Iran: Kermanshah prov., stream Golain at Sare-Baghe-Golain
G. pallens	A	MZ959039 [XXIII]			35.160	46.339		Iran: Kermanshah prov., Sirvan River at Hajij
G. pallens	C		G511b [XXIII]	G511R [XXIII]	35.118	46.257	19	Iran: Kermanshah prov., Sirwan River
G. pallens	A	MZ959040			34.645	46.286		Iran: Kermanshah prov., stream Zemkan 3 km north of Zamkan-e Olya

2.2. Material Examined in the Morphological Analyses

All from Iran.

Glyptothorax alidaeii: ZM-CBSU H901, 17, 50–107 mm SL, Kohgiluyeh and Boyer-Ahmad Prov.: Beshar River, 30°40′33.6″ N 51°31′57.0″ E. ZM-CBSU H997, 5, 113–149 mm SL, Lorestan Prov.: Kashkan River, 33°27′30.0″ N 47°55′46.8″ E. ZM-CBSU H981, 14, Ilam Prov.: Seimare River, 33°40′46.7″ N 47°03′19.1″ E.

Glyptothorax cous: ZM-CBSU H974, 1, 97.9 mm SL & ZM-CBSU H982, 1, 68.4 mm SL, Ilam Prov.: Seimareh River at Cham Namesht, 33°10′57.5″ N 47°25′00.2″ E. BMNH 1955.6.25.2, 243 mm SL; Syria: Coic (Qweiq) River (photographs only).

Glyptothorax galaxias: ZM-CBSU H976, 5, 27.6–72.2 mm SL, Kermanshah Prov.: Kharchang River, a tributary of Gamasiab River, 34°22′14.9″ N 47°54′43.7″ E; ZM-CBSU H975, 1, 76.3 mm SL, Ilam Prov.: Chardavol, a tributary of Seimare River, 33°41′35.0″ N 46°42′56.2″ E.

Glyptothorax hosseinpanahii: ZM-CBSU H918–H941 & H967–H973, 31, 47–82 mm SL, Fars Prov.: Fahlian River at Berim bridge in Kopen Village, 30°19′41.0″ N 51°15′04.0″ E.

Glyptothorax silviae: ZM-CBSU H955, 12, 33.5–64.9 mm SL, Khuzestan Prov.: Ab-e Aala River at Zard-e Mashin Village, 31°22′33.5″ N 49°43′47.7″ E.

Glyptothorax shapuri: ZM-CBSU H918, 24, & H967, 7, 47–82 mm SL, Fars Prov.: Kohmareh Sorkhi stream, Helleh basin, 29°23′39.6″ N 52°09′39.8″ E.

2.3. DNA Extraction and PCR

Total genomic DNA was extracted from fin clips using a salt method protocol described in Bruford et al. [7]. Polymerase chain reaction (PCR) was used to amplify fragments of two

mtDNA genes, cytochrome c oxidase subunit 1 (COI) barcode region and Cytochrome b (*Cyt* b) and one nuclear locus, Recombination Activating 2 (RAG2). Primers, reaction profiles and cycling conditions were modified from Jiang et al. [8] and Zarei et al. [9] (Table S1). PCR amplifications were conducted in a total volume of 25 µL (including 12.5 µL of a ready 2X Taq PCR Master Mix (ParstousTM), 0.5 µL of each primer (10 pmol/µL), 6 µL of the target DNA and 5.5 µL DNase-free distilled water). Automated Sanger sequencing of purified PCR products was performed using ABI Prism R BigDyeTM Terminator v. 3.1 chemistry (Applied Biosystems, Foster City, CA, USA) on an Applied BiosystemsTM ABI PRISM 3730xl by Macrogen, South Korea.

2.4. Additional Sequence Data

In addition to the newly determined DNA sequences from Iran (25 COI, 24 *Cyt* b and 17 RAG2 sequences) and Turkey (4 COI sequences), we used 64 previously published and georeferenced COI barcode sequences from 10 *Glyptothorax* species from Iran and Turkey (i.e., *G. pallens*, *G. kurdistanicus*, *G. daemon*, *G. daemon*, *G. cous*, *G. armeniacus*, *G. galaxias*, *G. silviae*, *G. shapuri*, *G. alidaeii* and *G. hosseinpanahii*) obtained from GenBank and ZFMK and derived from the works of Freyhof et al. [4] and Mousavi-Sabet et al. [5] (Table 1). For the multilocus phylogenetic analysis, also additional COI, *Cyt* b and RAG2 sequences of 21 *Glyptothorax* species from different Asian localities and derived from the works of Jiang et al. [8] and Sullivan et al. [10] were obtained from GenBank (Table S2). *Bagarius yarrelli* (Sisoridae) from Chen et al. [11] and Peng et al. [12] was used as outgroup.

2.5. Phylogenetic Analyses

BioEdit 7.0.4 [13] was used to read and edit the DNA chromatograms. All novel DNA sequences including 29 COI, 24 *Cyt* b and 17 RAG2 sequences were deposited in GenBank (accession numbers and details of the specimens are given in Table S3: COI: OP585111–OP585139; *Cyt* b: OP589359–OP589381; RAG2: OP589382–OP589398) and the collection sites of the Middle Eastern *Glyptothorax* samples used in this study are illustrated in Figure 1. The DNA sequences were aligned using the ClustalW algorithm implemented in MEGA 7 [14]. After having trimmed out the sequences tails, the alignment of the novel fragments and those downloaded from GenBank led to trimmed aligned fragments of 651 bp (COI), 989 bp (*Cyt* b) and 892 bp (RAG2). The nucleotide substitution models best fitting the COI, *Cyt* b and RAG2 sequences were selected using the Akaike information criterion (AIC) [15] in JModelTest 2.1.3 [16]. The saturation test of Xia et al. [17] in DAMBE 7 [18] was used to test the nucleotide substitution saturation in the sequences. The fragments of both the mitochondrial and nuclear-selected markers were concatenated in a single partitioned dataset (2532 bp). Phylogenetic analyses of the partitioned concatenated dataset including the fragments of the amplified DNA markers were conducted using the software packages MrBayes v. 3.2.6 [19] and RaxML 7.2.5 (10,000 bootstrap replicates) [20] to infer the phylogenetic relationships through Bayesian Inference (BI) and Maximum Likelihood (ML) analyses. As support measures for the nodes, bootstrap values (BPs) [21] were calculated with 1000 replicates in the ML trees, whereas the node posterior probability (PP) values were reported in the BI trees. In the BI analyses, two independent Markov Chain Monte Carlo analyses were performed with 30 million generations (25% as burn-in). Convergence in the analysis was reached (effective sample size (ESS) >200 in all the analyses performed).

2.6. Molecular Species Delimitations

To delineate "molecular species", we used four molecular species delimitation methods on the COI dataset: (i) two distance-based methods, the Automatic Barcode Gap Discovery (ABGD) [22] and Assemble Species by Automatic Partitioning method (ASAP) [23]; (ii) a network-based method, the reversed Statistical Parsimony (SP) [24]; and (iii) a topology-based method, the multiple-rate Bayesian Poisson Tree Process (mPTP) [25]. We tested the COI dataset on the ABGD webserver (https://bioinfo.mnhn.fr/abi/public/abgd/ (accessed on 28 February 2022)) with a combination of ABGD settings within a parameter

range of P_{min} = 0.001, P_{max} = 0.1 and a gap width of 1.1, all for a total of 10 steps. ASAP was run through its web interface (https://bioinfo.mnhn.fr/abi/public/asap/asapweb.html (accessed on 28 February 2022)) using the Kimura (K80) ts/tv (=0.2). TCS 1.21 [26] was used to calculate a Statistical Parsimony (SP) network, using a 95% connection probability threshold to delineate molecular species. The mPTP server (https://mptp.h-its.org (accessed on 28 February 2022)) was used with a Bayesian topology produced in MrBayes as an input tree and the analysis was run under default settings. Estimates of genetic divergence between the Middle Eastern species/lineages of *Glyptothorax* were calculated using the K2P model implemented in MEGA 7. PopART 1.7 [27] was used to investigate the phylogenetic depth and evolutionary relationships among haplotypes based on the median-joining (MJ) method.

3. Results

3.1. Phyleogenetic Placements and Molecular Species Delimitations

The final COI alignment of *Glyptothorax* from the Middle East included 29 novel (25 sequences from 21 Iranian localities and 4 sequences from 3 localities in Turkey) and 64 previously published sequences derived from Freyhof et al. [4] and Mousavi-Sabet et al. [5], trimmed to 651 bps. The nucleotide substitution pattern showed that the COI sequences have not reached substitution saturation (*Iss* < *Iss.cS* and *Iss* < *Iss.cA*) and are, therefore, well applicable for phylogenetic analysis (Table S4). Based on a General Time-Reversible model of sequence evolution with a gamma-distributed rate variation among sites (GTR+G), this dataset was analyzed using the BI and ML methods (Figure 2), resulting in a phylogeny with 11 major clades corresponding to 10 nominal species: *G. pallens*, *G. kurdistanicus*, *G. armeniacus*, *G. galaxias*, *G. silviae*, *G. shapuri*, *G. alidaeii*, *G. hosseinpanahii*, *G. cous* and *G. daemon*. *Glyptothorax daemon* is separated into two mitochondrial lineages (hereafter, *G. daemon* 1 and *G. daemon* 2). According to Freyhof et al. [4], *G. daemon* 2 may represent a hybrid population between *G. cous* and *G. daemon* 1. Most of the nodes within the genealogy are supported with high PB and BP values. The deepest split in this genealogy is between *G. pallens*, followed by *G. kurdistanicus* and the remainder of the species. The next diverging clade contains *G. cous* and the two lineages of *G. daemon*. All the Iranian endemic members of the genus *Glyptothorax*, except for *G. pallens* (i.e., *G. galaxias*, *G. silviae*, *G. shapuri*, *G. alidaeii* and *G. hosseinpanahii*) form a monophyletic clade and are more derived than other species. *Glyptothorax armeniacus*, an endemic catfish to the headwater streams in the Euphrates drainage (Türkiye), is the sister group of this Iranian endemic clade.

The nucleotide substitution pattern also confirmed that the *Cyt* b and RAG2 sequences (24 and 17 novel sequences from Iran, respectively) have not reached substitution saturation (*Iss* < *Iss.cS* and *Iss* < *Iss.cA*) and are, therefore, well applicable for phylogenetic analyses (Table S4). The best-fit nucleotide substitution models for these loci were GTR+I+G and SYM+G, respectively. The combined COI+*Cyt* b (Figure 3a) and COI+*Cyt* b+RAG2 (Figure 3b) trees for the Iranian species with high support values (PP and BP) retrieved similar results with the topology from the COI tree. The deepest split is between *G. pallens* and the remainder of the species; the next diverging clade contains *G. kurdistanicus* and *G. cous*, followed by *G. galaxias* as the sister group of the remainder of the species. *Glyptothorax hosseinpanahii* and *G. alidaeii* formed a clade sister to another clade containing *G. silviae* and *G. shapuri*.

The molecular trees (Figures 2 and 3) show that the new specimens collected from Iran at the Kohmareh Sorkhi stream and the Dalaki River belong to *G. shapuri*, at the Ab-e Aala and Maroun rivers belonging to *G. silviae*, at the Fahlian River belonging to *G. hosseinpanahii*, at the Khersaan, Beshar, Armand and Kashkan rivers and Bibi Seyedan (Isfahan) belonging to *G. alidaeii*, at the Gamasiab and Chardaval rivers, Khak Daneh (Isfahan) and Kata (Kohgiluyeh and Boyer-Ahmad) belonging to *G. galaxias*, at the Sirvan River belonging to *G. kurdistanicus* and *G. pallens* and at the Seimare River (Ilam) belonging to *G. cous*, which represents the first record of *G. cous* in Iranian waters. The updated distributional ranges of these species based on molecular data are depicted in Figure 1, which highlights: (i) the

significantly wider distributional ranges for *G. galaxias* and *G. alidaeii* and (ii) sympatric presence of *G. galaxias* and *G. alidaeii* in the upper Karun drainage, *G. galaxias*, *G. alidaeii* and *G. cous* in the upper Karkheh drainage and *G. pallens* and *G. kurdistanicus* in the tributaries of the Sirvan River.

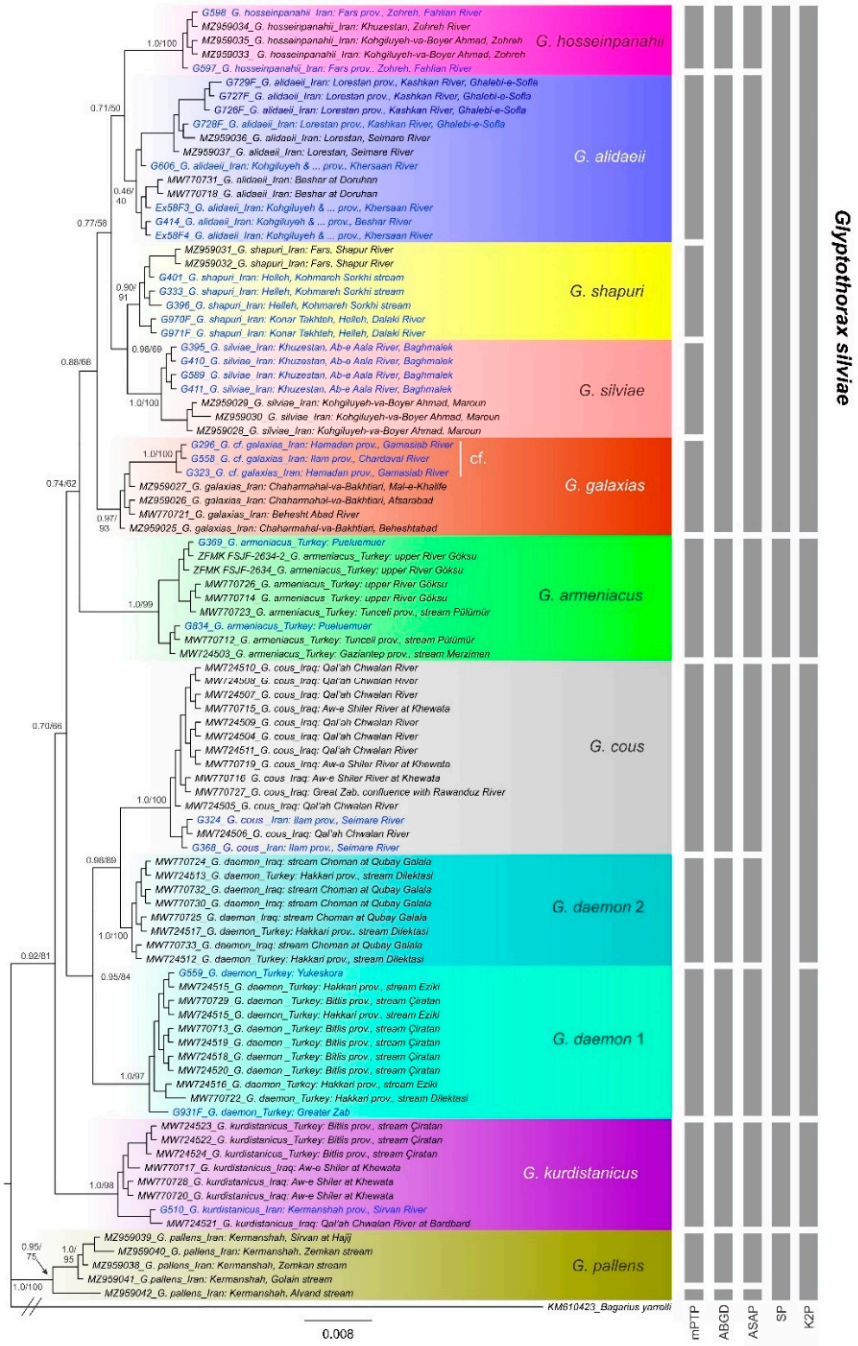

Figure 2. Bayesian (BI) and Maximum Likelihood (ML) tree of the genus *Glyptothorax* from the Middle East based on COI dataset, showing the phylogenetic placements of the new samples from Iran and Turkey (taxa with a blue font) and results of five molecular species delimitation methods (gray bars on the right): mPTP, multiple-rate Poisson Tree Process; ABGD, Automatic Barcode Gap Discovery; ASAP, Assemble Species by Automatic Partitioning; SP, reversed Statistical Parsimony; K2P, species delimitation based on the K2P distance new species threshold value (i.e., 2%). Support values are indicated beside the nodes [BI posterior probability/ML bootstrap (PP/BP)].

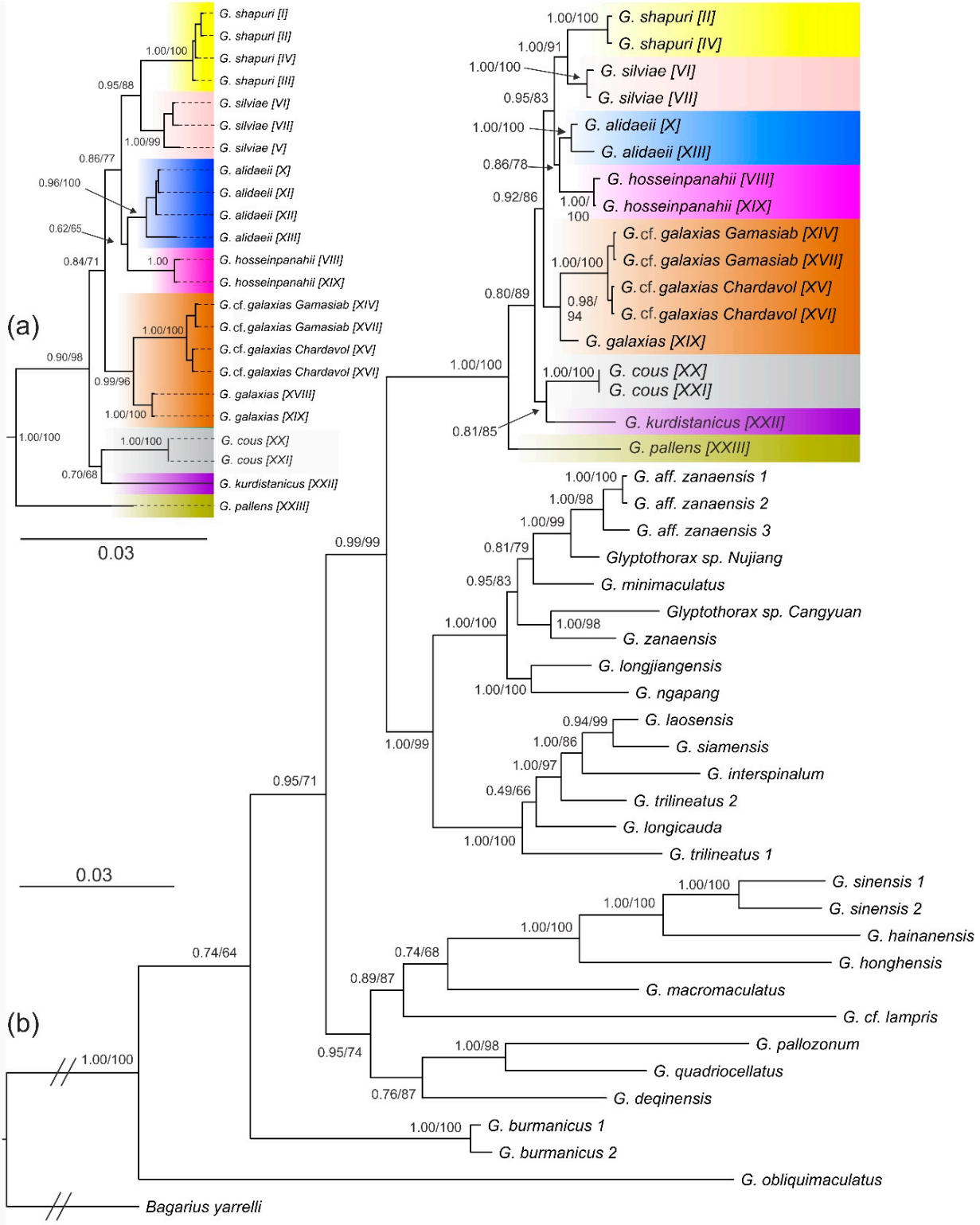

Figure 3. Phylogenetic relationships within *Glyptothorax* with focus on the Middle Eastern species, obtained from Bayesian (BI) and Maximum Likelihood (ML) analyses of combined COI+*Cyt* b (**a**) and COI+*Cyt* b+RAG2 (**b**) datasets. Support values given as Bayesian posterior probability/ML bootstrap (PP/BP). Greek numbers (I–XXIII) refer to the combined sequences from Table 1.

The four conceptually different molecular species delimitation methods revealed 5–12 molecular species in a COI dataset comprising 93 sequences, belonging to 10 nominal species (Figure 2). SP was the most conservative method, as it delineated five molecular

species. Out of 10 nominal species, 3 species (i.e., *G. pallens*, *G. kurdistanicus* and *G. armeniacus*) were delimited through the SP tool. It grouped *G. daemon* (including *G. daemon* 1 and *G. daemon* 2) and *G. cous* and all members of the Iranian endemic clade (i.e., *G. galaxias*, *G. silviae*, *G. shapuri*, *G. alidaeii* and *G. hosseinpanahii*) into single molecular entities. The ABGD and ASAP methods similarly delineated nine molecular species. Out of 10 nominal species, 4 species (i.e., *G. kurdistanicus*, *G. cous*, *G. armeniacus* and *G. hosseinpanahii*) were delimited through these tools. Both analyses presented potential species-level diversity in *G. pallens* (one in the Alvand stream and the other in the Siravan River, the Golain and Zemkan streams) and *G. daemon* (one as *G. daemon* 1 and the other as *G. daemon* 2). Both methods pooled all species of the Iranian endemic clade, except for *G. hosseinpanahii* (i.e., *G. galaxias*, *G. silviae*, *G. shapuri*, *G. alidaeii*), into a single molecular species. The mPTP method delineated 12 molecular species. Out of 10 nominal species, 8 species (i.e., *G. kurdistanicus*, *G. cous*, *G. armeniacus*, *G. galaxias*, *G. silviae*, *G. shapuri*, *G. alidaeii* and *G. hosseinpanahii*) were delimited through this tool. Similar to ABGD and ASAP, mPTP presented potential species-level diversity in *G. pallens* and *G. daemon*. In addition, species delimitation based on the K2P genetic distance new species threshold value (i.e., 2%: [28]) only provided support for six molecular species (Table 2, Figure 2). Out of 10 nominal species, 3 species (i.e., *G. pallens*, *G. kurdistanicus* and *G. armeniacus*) were delimited through the K2P method. It lumped *G. daemon* 2 and *G. cous* and all members of the Iranian endemic clade into single molecular entities.

Table 2. Estimates of K2P genetic divergence (%) between different species of *Glyptothorax* from the Middle East (lower left matrix). Values lower than 2% are shown in bold. Standard deviations (SDs) are shown above the diagonal.

		1	**2**	**3**	**4**	**5**	**6**	**7**	**8**	**9**	**10**	**11**
1	*G. galaxias* †		0.50	0.39	0.50	0.36	0.68	0.60	0.56	0.46	0.64	0.62
2	*G. silviae*	2.06		0.37	0.54	0.43	0.72	0.63	0.59	0.57	0.66	0.68
3	*G. shapuri*	**1.40**	**1.22**		0.50	0.36	0.63	0.63	0.53	0.53	0.61	0.62
4	*G. hosseinpanahii*	**1.97**	**1.97**	**1.76**		0.47	0.71	0.66	0.66	0.61	0.73	0.69
5	*G. alidaeii*	**1.43**	**1.66**	**1.30**	**1.73**		0.60	0.56	0.57	0.50	0.61	0.55
6	*G. pallens*	3.45	3.81	3.27	3.71	2.98		0.68	0.68	0.63	0.83	0.65
7	*G. cous*	2.38	2.77	2.89	3.00	2.37	3.55		0.61	0.43	0.74	0.63
8	*G. daemon* 1	2.32	2.85	2.32	3.08	2.76	3.96	2.61		0.50	0.71	0.70
19	*G. daemon* 2 ‡	**1.44**	2.28	2.08	2.51	**1.88**	3.05	**1.10**	**1.80**		0.70	0.64
10	*G. armeniacus*	2.93	2.93	2.69	3.49	2.67	4.37	3.65	3.71	3.16		0.69
11	*G. kurdistanicus*	2.71	3.25	2.72	3.16	2.44	3.56	2.84	3.32	2.75	3.48	

† Including *G.* cf. *galaxias*; ‡ a possible hybrid population (Freyhof et al. [4]).

The median-joining (MJ) haplotype networks for COI and *Cyt* b in Figure 4 show the number of mutational steps and phylogeographic depth between the observed haplotypes of *Glyptothorax* from the Middle East. They further show marked divergences within two species: (i) *G. pallens*: divergence between the Alvand stream and the Siravan River, the Golain and Zemkan streams haplotypes (deviated by nine mutational steps = 1.5% K2P genetic divergence in COI), (ii) *G. galaxias*: divergence between the upper Karun drainage (*G. galaxias*) and the upper Karkheh drainage (*G.* cf. *galaxias*) haplotypes (deviated by six and thirteen mutational steps in their COI and *Cyt* b sequences, respectively).

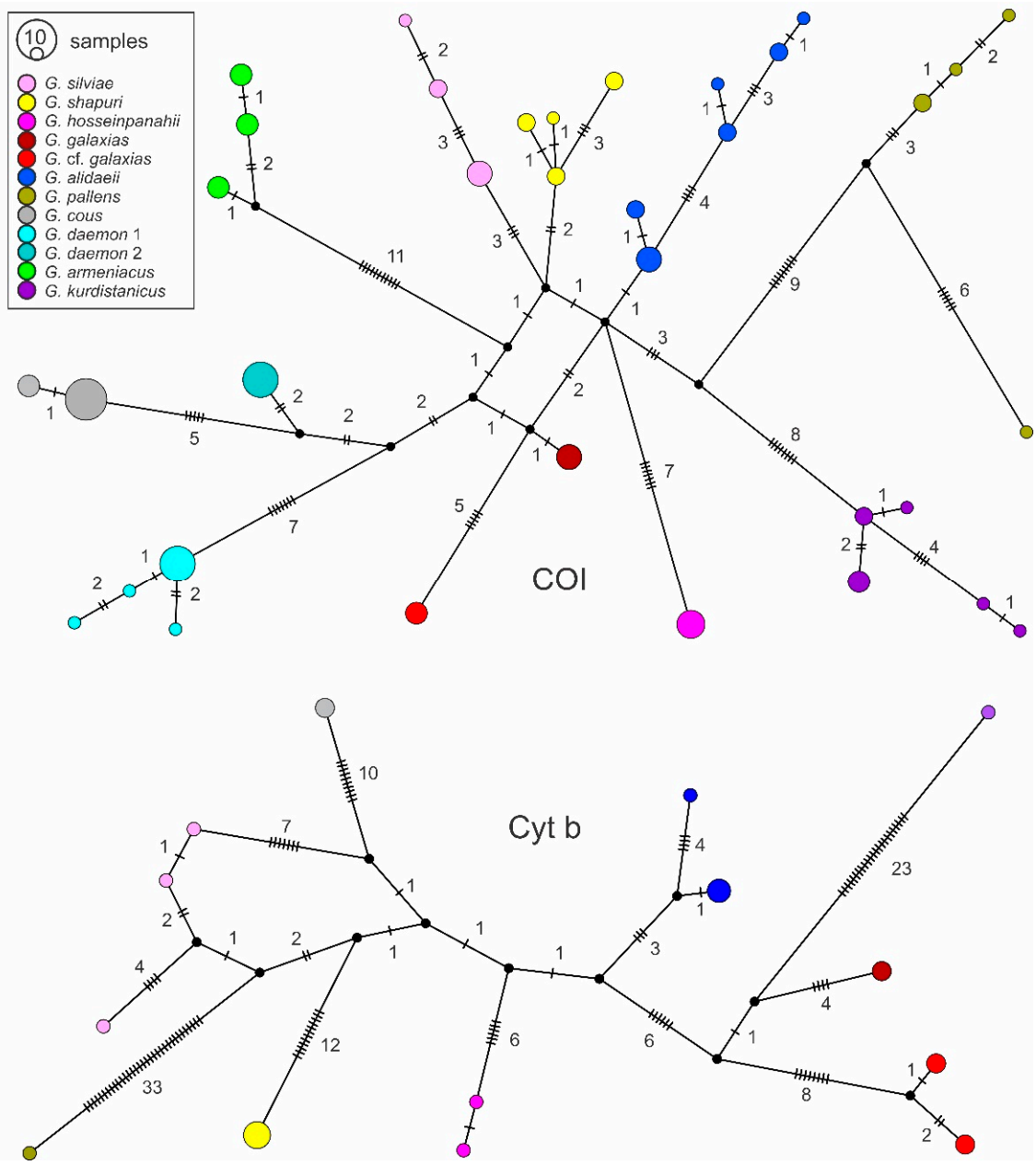

Figure 4. Median-joining (MJ) haplotype networks of mitochondrial COI and *Cyt* b haplotypes of *Glyptothorax* spp. from the Middle East. Circle sizes depict proportions of haplotypes, the smallest corresponds to one. Small black circles correspond to missing/hypothetical haplotypes. Hatch marks/numbers represent mutational steps between neighboring haplotypes.

3.2. Morphological Results

3.2.1. The Name-Bearing Iranian Endemic Clades

See Figures 5 and 6 for general appearance and Table 3 for morphometric data of studied populations. The holotype general morphology of *G. silviae* is illustrated in Figure 7. As the morphological description of new Iranian species was mainly based on the thoracic adhesive apparatus (e.g., anteromedial striae), length of maxillary, inner mandibular and outer mandibular barbels and the caudal fin shape, the mentioned characters and several others were studied. Based on the data given in Table 3 and Figures 5 and 6, these characters show inter- and intra-population variation in closely related species (i.e., *G. alidaeii*, *G. galaxias*, *G. hosseinpanahii*, *G. shapuri* and *G. silviae*).

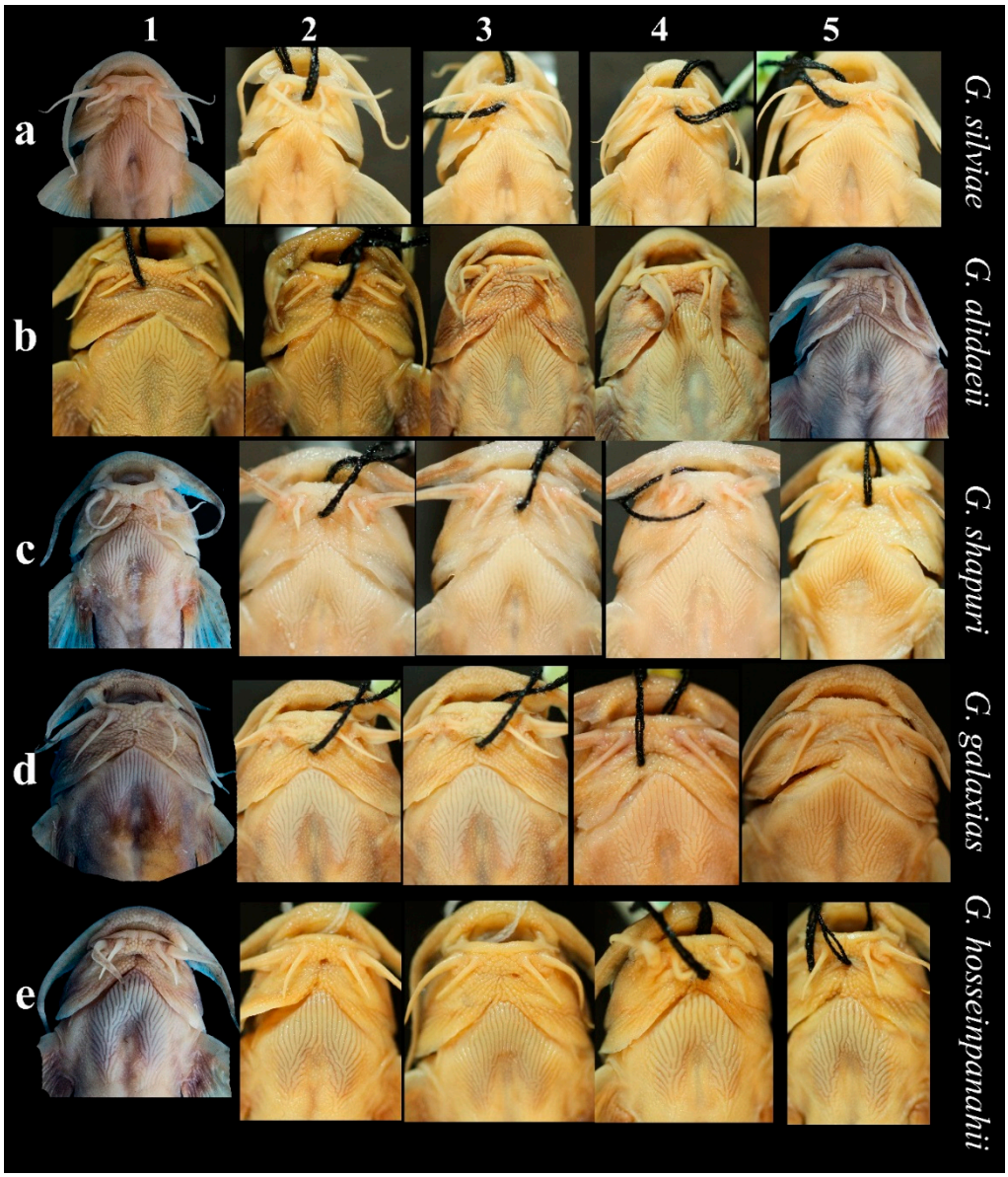

Figure 5. *Glyptothorax* spp. thoracic adhesive apparatus, (**a1**), ZM-CBSU H959, 55 mm SL; (**a2**), ZM-CBSU H961, 41 mm SL; (**a3**), ZM-CBSU H964, 45 mm SL; (**a4**), ZM-CBSU H965, 54 mm SL; (**a5**), ZM-CBSU H966, 65 mm SL; Ab e Aala R.; (**b1**), ZM-CBSU H902, 94 mm SL; (**b2**), ZM-CBSU H903, 68 mm SL; Bashar R.; (**b3**), ZM-CBSU 4, 134 mm SL; (**b4**), ZM-CBSU 3, 142 mm SL; (**b5**), ZM-CBSU H997, 113 mm SL; Kashkan R.; (**c1**), ZM-CBSU H970, 70 mm SL; (**c2**), ZM-CBSU H939, 54 mm SL; (**c3**), ZM-CBSU H940, 52 mm SL; (**c4**), ZM-CBSU H941, 55 mm SL; (**c5**), ZM-CBSU H968, 74 mm SL; Kohmareh Sorkhi R.; (**d1**), ZM-CBSU H979, 72 mm SL; (**d2**), ZM-CBSU H980, 64 mm SL; (**d3**), ZM-CBSU H978, 65 mm SL; (**d4**), ZM-CBSU H976, 67 mm SL; Gamasiab River.; (**d5**), ZM-CBSU H975, 76 mm SL; Chardavol R.; (**e1**), ZM-CBSU H949, 72 mm SL; (**e2**), ZM-CBSU H945, 55 mm SL; (**e3**), ZM-CBSU H946, 67 mm SL; (**e4**), ZM-CBSU H947, 85 mm SL; (**e5**), ZM-CBSU H951, 65 mm SL; Fahlian R.

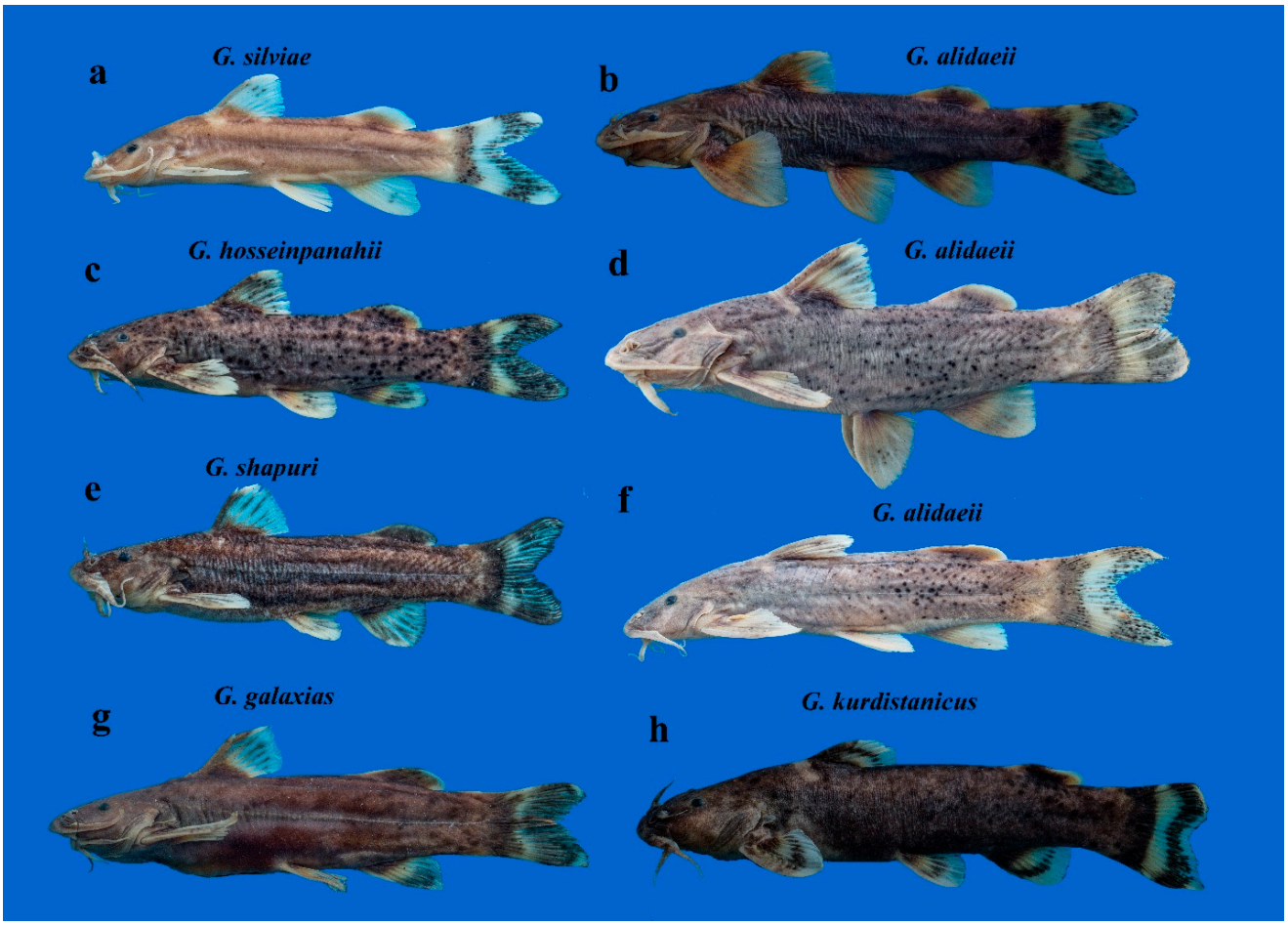

Figure 6. *Glyptothorax* spp. (**a**), ZM-CBSU H959, 55.2 mm SL; Ab e Aala R.; (**b**), H903, 68.4 mm SL; Bashar R.; (**c**), H949, 71.5 mm SL; Fahlian R.; (**d**), H997, 112.6 mm SL; Kashkan R.; (**e**), H970, 70 mm SL; Kohmareh Sorkhi R.; (**f**), H983, 90.2 mm SL; Seimareh R.; (**g**), H979, 72.2 mm SL; Gamasiab R.; (**h**), 1256/5, 92 mm SL; Sirvan R.

Table 3. Morphometric data of *Glyptothorax alidaeii* (ZM-CBSU H901, Bashar River, *n* = 8; ZM-CBSU H983, Seimare River, *n* = 9; ZM-CBSU H997, Kashkan River, *n* = 5), *G. galaxias* (ZM-CBSU H975, Gamasiab River, *n* = 6), *G. hosseinpanahii* (ZM-CBSU H942, Fahlian River, *n* = 10), *G. shapuri* (ZM-CBSU H918, Kohmareh Sorkhi River, *n* = 16), *G. silviae* (ZM-CBSU H955, Ab-e Aala River, *n* = 9) and *G. cous* (ZM-CBSU H974, H982, *n* = 2).

Species	***G. alidaeii***		***G. galaxias***		***G. hosseinpanahii***	
	Range	**Mean ± SD**	**Range**	**Mean ± SD**	**Range**	**Mean ± SD**
SL	59.7–148.8	100.2	27.6–76.3	62.1	46.8–71.5	62.5
% SL						
HL	24.1–27.0	25.4 ± 0.8	25.6–30.3	27.7 ± 1.6	25.3–27.2	26.3 ± 0.6
Pdl	32.8–37.9	35.3 ± 1.7	34.1–40.9	37.1 ± 2.4	34.6–36.8	35.6 ± 0.6
Pol	68.4–82.2	77.4 ± 3.4	70.1–78.7	74.7 ± 3.5	73.8–79.6	76.3 ± 1.6
Dl	10.8–14.9	13.1 ± 0.9	10.1–13.9	12.3 ± 1.2	11.5–14.2	12.6 ± 0.9
Dd	18.0–25.6	21.2 ± 1.8	19.4–23.9	21.1 ± 1.6	19.9–23.0	21.3 ± 0.9
Al	10.9–14.2	12.5 ± 1.0	11.1–14.8	12.7 ± 1.6	11.2–13.8	12.2 ± 0.9
Ad	18.6–23.5	21.2 ± 1.6	20.2–24.2	22.2 ± 1.5	19.8–24.0	21.1 ± 1.2

Table 3. *Cont.*

Species	*G. alidaeii*		*G. galaxias*		*G. hosseinpanahii*	
	Range	**Mean ± SD**	**Range**	**Mean ± SD**	**Range**	**Mean ± SD**
Pal	66.0–74.5	69.2 ± 2.0	70.3–73.3	71.8 ± 1.3	66.9–71.3	69.5 ± 1.3
Pl	23.1–28.3	25.3 ± 1.4	22.8–24.9	23.9 ± 0.9	23.9–26.8	25.1 ± 0.9
Vl	15.6–18.9	17.2 ± 0.9	16.0–17.1	16.5 ± 0.5	16.4–18.1	16.9 ± 0.5
Pvl	47.4–54.6	51.6 ± 1.7	53.4–61.0	55.8 ± 2.7	50.1–53.4	51.5 ± 0.9
Mxd	17.1–25.5	19.8 ± 2.4	18.6–23.7	21.2 ± 2.2	18.7–22.3	20.1 ± 1.2
Mid	10.9–15.0	13.1 ± 1.1	13.0–16.4	14.7 ± 1.2	11.7–13.0	12.6 ± 0.4
PV	28.4–40.1	32.2 ± 2.7	32.3–38.5	34.5 ± 2.4	29.8–31.7	30.7 ± 0.5
VA	15.9–21.0	18.3 ± 1.4	13.6–19.3	16.3 ± 2.1	14.9–18.9	17.6 ± 1.2
DAd	6.2–17.2	13.4 ± 2.5	7.9–14.7	11.8 ± 2.6	9.4–14.1	11.8 ± 1.7
Cl	22.7–32.0	27.2 ± 2.7	21.2–30.8	25.0 ± 3.3	26.1–30.9	27.9 ± 1.2
Cp	15.4–23.5	20.5 ± 2.4	18.7–20.5	19.5 ± 0.7	19.8–22.2	20.8 ± 0.7
CPI	1.2–1.8	1.6 ± 1.4	1.2–1.6	1.3 ± 0.1	1.6–1.7	1.6 ± 0.0
TAI	1.1–1.6	1.3 ± 0.1	1.0–1.4	1.2 ± 0.1	1.2–1.5	1.3 ± 0.1
Adl/DAd	1.3–3.6	1.8 ± 0.5	1.6–2.7	1.9 ± 0.5	1.5–2.4	1.8 ± 0.3
% HL						
Hd	50.4–67.9	61.1 ± 4.4	52.1–71.7	61.7 ± 7.8	54.0–72.1	62.5 ± 6.0
Hw	75.9–90.5	84.2 ± 3.7	87.6–93.2	90.6 ± 2.3	58.2–83.4	79.1 ± 7.4
Pr	46.0–56.3	52.8 ± 3.1	41.9–49.0	46.7 ± 2.7	50.2–59.4	53.0 ± 2.6
Po	35.0–44.7	40.3 ± 2.5	43.3–47.3	45.1 ± 1.6	36.1–50.5	40.1 ± 4.1
I	20.7–32.2	25.6 ± 2.3	26.6–31.1	28.5 ± 1.6	25.2–31.1	27.5 ± 1.9
E	8.0–12.1	10.0 ± 1.2	7.3–10.9	9.2 ± 1.2	6.3–11.2	8.3 ± 1.5
Mw	25.7–36.1	29.8 ± 2.7	30.5–35.2	33.1 ± 1.8	26.4–35.2	30.2 ± 2.9
Nbl	25.5–38.2	30.4 ± 3.4	37.5–49.4	44.3 ± 4.3	28.3–37.1	32.0 ± 2.4
Mbl	78.3–121.5	95.4 ± 10.0	79.2–94.8	86.2 ± 5.9	88.0–100.7	95.5 ± 3.9
Omb	42.3–67.1	54.4 ± 7.6	56.1–60.1	57.9 ± 1.3	48.8–57.6	52.0 ± 2.8
Imb	22.6–39.3	29.9 ± 4.6	31.6–36.6	34.3 ± 1.8	26.2–29.5	27.8 ± 1.2
	G. shapuri		*G. silviae*		*G. cous*	
	Range	**Mean ± SD**	**Range**	**Mean ± SD**	**Range**	**Mean ± SD**
SL	50.6–81.4	65.5	33.5–64.9	47.4	68.4–97.9	83.1
% SL						
HL	24.7–28.1	26.3 ± 1.0	26.6–28.9	27.8 ± 0.9	31.0–31.4	31.2 ± 0.3
Pdl	33.6–36.8	35.1 ± 1.0	35.2–37.9	36.4 ± 1.0	38.6–40.8	39.7 ± 1.6
Pol	75.0–82.4	77.3 ± 1.8	79.4–82.8	81.1 ± 1.0	71.2–71.2	71.2 ± 0.3
Dl	12.0–15.7	13.6 ± 1.0	11.5–13.2	12.3 ± 0.6	13.1–13.4	13.3 ± 0.2
Dd	18.2–22.1	20.0 ± 1.2	21.1–23.6	22.2 ± 0.7	21.3–24.2	22.7 ± 2.0
Al	11.4–13.9	12.4 ± 0.6	10.6–14.4	11.8 ± 1.2	13.0–13.3	13.2 ± 0.2
Ad	18.7–21.1	19.8 ± 0.7	21.3–22.9	22.0 ± 0.5	21.2–21.4	21.3 ± 0.1
Pal	66.4–70.8	68.1 ± 1.3	68.2–70.5	69.1 ± 0.8	69.9–72.1	71.0 ± 1.6
Pl	21.5–25.6	23.5 ± 1.1	24.2–26.9	25.8 ± 0.7	20.6–24.2	22.4 ± 2.5

Table 3. *Cont.*

	G. shapuri		*G. silviae*		*G. cous*	
	Range	**Mean ± SD**	**Range**	**Mean ± SD**	**Range**	**Mean ± SD**
Vl	14.0–17.5	15.8 ± 0.9	16.4–18.3	17.2 ± 0.7	15.0–17.1	16.0 ± 1.5
Pvl	48.6–54.0	51.1 ± 1.4	50.2–53.9	52.3 ± 1.3	55.5–56.4	56.0 ± 0.6
Mxd	18.2–21.5	19.9 ± 1.2	15.9–19.5	17.1 ± 1.2	18.7–19.3	19.0 ± 0.4
Mid	11.5–15.2	13.4 ± 0.9	10.2–13.1	11.4 ± 0.8	8.7–9.1	8.9 ± 0.3
PV	26.0–33.3	30.4 ± 1.7	27.2–31.1	30.1 ± 1.4	32.0–33.3	32.7 ± 0.9
VA	15.8–18.6	17.4 ± 0.9	14.8–17.5	16.0 ± 1.0	16.9–18.6	17.7 ± 1.2
DAd	10.4–17.0	14.7 ± 1.7	10.9–14.5	13.1 ± 1.2	10.7–10.7	10.7 ± 0.5
Cl	24.5–30.0	26.7 ± 1.5	27.2–29.9	28.5 ± 0.9	25.4–25.5	25.4 ± 0.1
Cp	20.4–23.3	22.0 ± 0.9	19.6–21.7	20.6 ± 0.6	16.9–17.7	17.3 ± 0.6
CPI	1.5–1.8	1.6 ± 0.1	1.6–2.0	1.8 ± 0.1	1.9–2.0	1.9 ± 0.1
TAI	1.0–1.2	1.1 ± 0.1	1.0–1.2	1.5 ± 0.1	1.0–1.1	1.1 ± 0.1
Adl/DAd	1.1–2.2	1.4 ± 0.3	1.5–2.1	1.7 ± 0.2	2.0–2.0	2.0 ± 0.1
% HL						
Hd	53.8–71.9	61.7 ± 4.4	47.1–53.4	50.9 ± 2.2	48.2–55.9	52.0 ± 5.4
Hw	73.1–84.6	80.5 ± 2.5	73.5–81.4	77.2 ± 2.4	77.0–82.2	79.6 ± 3.7
Pr	46.4–53.5	50.8 ± 2.2	48.6–54.0	51.1 ± 1.7	47.1–50.1	48.6 ± 2.1
Po	40.0–44.1	41.7 ± 0.9	36.6–40.5	38.7 ± 1.4	43.1–45.0	44.1 ± 1.3
I	21.9–28.3	26.4 ± 1.7	24.1–27.7	25.6 ± 1.1	23.9–24.9	24.4 ± 0.7
E	6.5–11.4	9.7 ± 1.1	7.4–9.7	8.8 ± 0.7	6.1–8.6	7.3 ± 1.8
Mw	26.4–33.3	29.7 ± 2.3	25.2–33.9	28.4 ± 2.5	37.4–40.1	38.8 ± 1.9
Nbl	27.7–38.6	33.0 ± 2.8	34.0–44.4	37.0 ± 3.3	34.3–35.2	34.7 ± 0.6
Mbl	87.9–109.4	96.1 ± 6.2	103.3–117.4	108.6 ± 5.2	78.5–85.6	82.0 ± 5.0
Omb	50.3–58.7	54.9 ± 2.6	54.4–65.1	59.0 ± 2.9	50.0–51.9	51.0 ± 1.3
Imb	23.6–30.8	26.5 ± 2.2	26.7–37.5	30.2 ± 3.2	26.5–29.2	27.8 ± 1.9

SL = standard length (mm); % SL = in percent of standard length; HL = head length; Pdl = pre-dorsal length; Pol = post-dorsal length; Dl = dorsal-fin length; Dd = dorsal-fin depth; Al = anal-fin length; Ad = anal-fin depth; Pal = pre-anal length; Pl = pectoral-fin length; Vl = pelvic-fin length; Pvl = pre-pelvic length; Mxd = maximum body depth; Mid = minimum body depth; PV = distance between pectoral and pelvic-fin; VA = distance between pelvic and anal-fin; Dad = distance between dorsal and adipose fin; Cl = length of caudal fin; Cp = length of caudal peduncle; CPI = caudal peduncle index (L/D); TAI = thoracic adhesive apparatus index (L/W); Adl/Dad = adipose fin length/distance between dorsal and adipose fin; % HL = in percent of head length; Hd = head depth; Hw = head width; Pr = pre-orbital distance; Po = post-orbital distance; I = inter-orbital width; E = eye diameter; Mw = mouth width; Nbl = nasal barble length; Mbl = maxillary barbel length; Omb = outer mandibular barbell length; Imb = inner mandibular barbell length.

***Glyptothorax silviae* Coad, 1981**

Glyptothorax silviae Coad, 1981:291.

CMNFI 1979-0390A, 67.6 mm SL, holotype (Figure 7); CMNFI 1979-0390B, 2, paratypes, 44–51 mm SL; Iran: Khuzestan prov.: stream 3 km south of Bagh-e Malek, a tributary to Rud-e Zard or Ab-e Ala, 31.48349.908.

Synonyms

Glyptothorax alidaeii Mousavi-Sabet, Eagderi, Vatandoust & Freyhof, 2021:459, Figures 7–10.
Glyptothorax galaxias Mousavi-Sabet, Eagderi, Vatandoust & Freyhof, 2021:462, Figures 11–14.
Glyptothorax hosseinpanahii Mousavi-Sabet, Eagderi, Vatandoust & Freyhof, 2021:468, Figures 15–18.
Glyptothorax shapuri Mousavi-Sabet, Eagderi, Vatandoust & Freyhof, 2021:477, Figures 23–26.

Figure 7. *Glyptothorax silviae*, CMNFI 1979-0390A, 67.6 mm SL, holotype; Iran: stream 3 km south of Bagh'e Malek, Persian Gulf basin.

Diagnosis: *Glyptothorax silviae* is a species with a large variation in morphological characteristics, such as length of barbels, shape of thoracic adhesive apparatus, caudal peduncle index, adipose-fin length and distance between the base of the last dorsal-fin ray and adipose-fin origin, which are used in the original descriptions of the four newly described species, *G. alidaeii*, *G. galaxias*, *G. hosseinpanahii* and *G. shapuri*. Based on the original description, *G. silviae* is distinguished from *G. alidaeii* and *G. shapuri* by having maxillary barbel as long as the head (90–110% HL vs. 76–89% HL); inner mandibular

barbel 45–48% HL (vs. 19–33%); outer mandibular barbel 67–74% HL (vs. 42–49%). It is also distinguished from *G. galaxias* and *G. hosseinpanahii* by having long and numerous (vs. short or absent) anteromedial striae in thoracic adhesive apparatus. Our data do not confirm these diagnostic features, *G. silviae* vs. *G. alidaeii* and *G. shapuri*: (maxillary barbel 103–117% HL vs. 78–121% HL); (inner mandibular barbell 27–37% HL vs. 23–39% HL) and (outer mandibular barbell 54–65% HL vs. 42–67% HL). There is also a variety in the size and number of anteromedial striae in thoracic adhesive apparatus of *G. silviae*, *G. galaxias* and *G. hosseinpanahii* (see Figure 5a,d,e). Therefore, our data confirm the synonymy of *G. alidaeii*, *G. galaxias*, *G. hosseinpanahii* and *G. shapuri with G. silviae*.

Glyptothorax silviae is generally distinct in having long, or approximately as wide as long, thoracic adhesive apparatus (vs. short in *G. kurdistanicus*); head and flank without tubercles (vs. present in *G. armeniacus* and *G. cous*) and warts (vs. present in *G. daemon*); upper head, back and flank with few or many dark-brown spots and/or blotches (vs. in *G. pallens*) and medial pit of thoracic adhesive apparatus without striae (vs. present in *G. steindachneri*).

Key to Iranian *Glyptothorax* species:

1a—Head and flank with tubercles; mouth width 37–40% HL ... ... *G. cous*.
1b—Head and flank without tubercles; mouth width 25–35% HL 2
2a—Upper head, back and flank without brown or black spots or blotches ... ... *G. pallens*.
2b—Upper head, back and flank with few or many, dark-brown spots and, or blotches (faded in some preserved individuals) 3
3a—Thoracic adhesive apparatus wider than long, as wide as long in juveniles (0.7–0.9-times longer than wide); adipose-fin short, its length 0.6–1.0-times larger than the distance between the base of last dorsal-fin ray and adipose-fin origin ... ... *G. kurdistanicus*.
3b—Thoracic adhesive apparatus longer than wide or as wide as long (1.0–1.6-times longer than wide); adipose-fin usually long, its length 1.1–3.6-times larger than the distance between the base of last dorsal-fin ray and adipose-fin origin ... ... *G. silviae*.

3.2.2. *Glyptothorax cous* (Linnaeus, 1766)

Silurus cous Linnaeus, 1766:504 (Figure 8).

Diagnosis. *Glyptothorax cous* is distinct in having large mouth width (37.4–40.1% HL), large dark-brown blotches and numerous cloudy spots on the body. Thoracic adhesive apparatus is almost as wide as long (1.0–1.1-times longer than wide), poorly delineated at its posterior margin, only partly situated on a shallow, horseshoe-shaped swelling, swelling absent in many adult individuals; head, back and flank usually have large, bony, striated and elongated tubercles (absent in some individuals).

General morphology. See Figure 8 for the general appearance of two collected specimens from the Seimareh River, Iran, and Figure 9 for the general morphology of the type specimen; morphometric data are given in Table 3. Body spindle-shaped, pre-ventral profile flat and pre-dorsal profile slightly arched; head depressed, with bluntly pointed snout tip and sub-terminal mouth and fleshy lips; upper jaw longer than lower jaw, eyes small; thorax and anterior portion of abdomen flattened ventrally with a conspicuous rhomboidal-shaped thoracic adhesive apparatus with a central pit, which is open caudally; barbels four pairs, the nasal reaches posterior margin of orbit and longer than inner mandibular, maxillary with broad bases, when straightened, extending beyond posterior end of pectoral fin base, outer mandibular reaches middle of pectoral fin base; dorsal fin is small and situated closer to the snout tip than to caudal fin, its posterior margin slightly curved, with two spines and $6\frac{1}{2}$ branched rays, spines smooth with no serrations; pectoral fin extending to vertical of origin of dorsal fin-base, with one spine and $8\frac{1}{2}$ branched rays, spine strong and broad with posterior serrations; pelvic fin-origin at level of behind posterior end of dorsal base and extending to the anus, with one spine and $5\frac{1}{2}$ branched rays; anterior margin of adipose dorsal gently sloping and its origin is over or slightly anterior to the origin of anal fin; anus with two spines and $7\frac{1}{2}$–$8\frac{1}{2}$ branched rays; caudal is quite deeply forked, lower lobe slightly longer; thoracic adhesive apparatus index (L/W) 1.0–1.1; caudal peduncle index

(L/D) 1.9–2.0; adipose fin length/distance between dorsal and adipose fin 1.98–2.04; head blunt, spade-shaped, 31.0–31.4% SL.

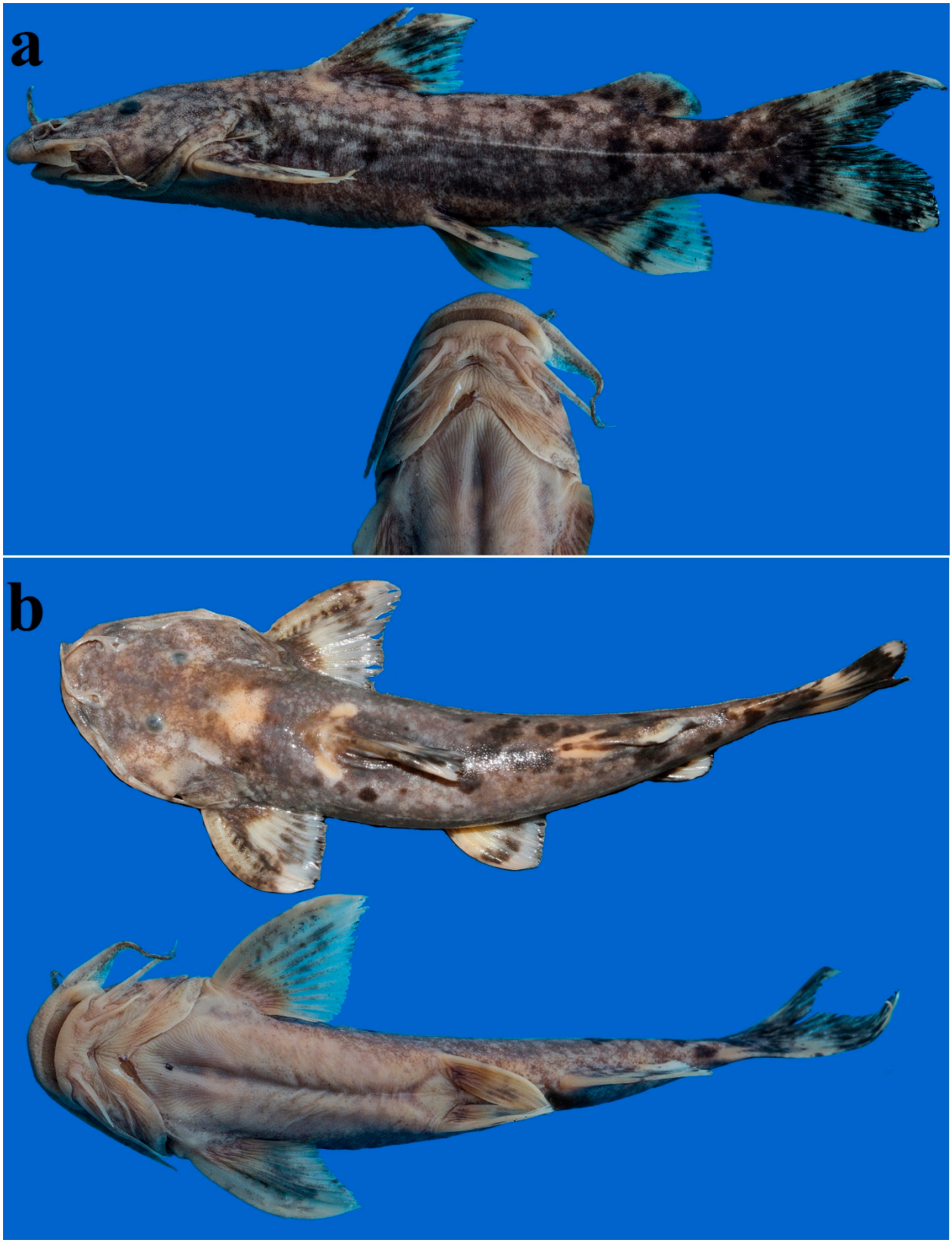

Figure 8. *Glyptothorax cous*, (**a**) ZM-CBSU H982, 68.4 mm SL; (**b**) ZM-CBSU H974, 98 mm SL; Iran: Seimareh River, Persian Gulf basin.

Figure 9. *Glyptothorax cous*, BMNH 1955.6.25.2, holotype, 243 mm SL; Syria: Qweiq at Aleppo. Copy right: The Trustees of the Natural History Museum, London.

Distribution. *Glyptothorax cous* is known from the Tigris and Euphrates River drainages in Iraq and Turkey. It is also known from the Seimareh River (Karkheh tributary), Cham Namesht, Persian Gulf basin in Iran, as a new record (Figure 1).

4. Discussion

The Iranian *Glyptothorax* species are taxonomically revised based on extensive geographic range and taxon sampling, tree topologies from mitochondrial COI and *Cyt* b and nuclear RAG2 markers (2532 bps), molecular species delimitation and genetic distance (K2P) analyses of DNA sequences against morphometric and morphological characters. All the Iranian endemic samples of *Glyptothorax*, following congruently well-supported BI and ML-based entities, formed six named molecular clades, i.e., *G. pallens*, *G. galaxias*, *G. silviae*, *G. shapuri*, *G. alidaeii* and *G. hosseinpanahii*. Only two groups were detected by the SP and K2P species delimitation approaches, i.e., *G. pallens* and the other Iranian endemic clades (i.e., *G. galaxias*, *G. silviae*, *G. shapuri*, *G. alidaeii* and *G. hosseinpanahii*) as the second group. However, a third group, *G. hosseinpanahii*, was detected by the ABGD and ASAP methods. Considering it as an independent species would render the rest of the second group a paraphyletic species. Therefore, the four molecular species delimitation methods combined with the BI and ML topologies (i.e., a majority rule consensus) consider all the Iranian endemic clades of *Glyptothorax*, except for *G. pallens*, as a single molecular entity. However, as there are not—and cannot be—any agreed universal thresholds for species delineation based on molecular data, we, as most other ichthyologists, usually adopt an iterative taxonomic approach [29]. This approach asks for the formulation of a testable species hypothesis and its testing by independent methods. If independent datasets (i.e., molecular data and morphology) agree in distinguishing two populations, these are recognized as valid species. We utilized our years of experience with the morphology of Iranian *Glyptothorax* populations and tried our best to perceive consistent morphological differences, but without success. We discuss this point in detail below.

Based on our available data to GF, Mousavi-Sabet et al. [5] described five new species of *Glyptothorax* from Iran. *Glyptothorax alidaeii*, *G. galaxias*, *G. hosseinpanahii* and *G. shapuri* are described based on low-genetic distances (<2%) and the overlapping morphological characters. However, due to the overlapping, we failed to distinguish these species based on the given morphometric characters. The morphological description of new species was mainly based on the thoracic adhesive apparatus (e.g., anteromedial striae), length of maxillary, inner mandibular and outer mandibular barbels and the caudal fin shape; however, these characters show inter- and intra-population variation in closely related species (i.e., *G. alidaeii*, *G. galaxias*, *G. hosseinpanahii*, *G. shapuri* and *G. silviae*). According to Mousavi-Sabet et al. [5], *G. silviae* is distinguished from *G. hosseinpanahii* by having the thoracic adhesive apparatus strongly elevated (vs. moderately elevated), without or with few short anteromedial striae (vs. many and long). However, as illustrated in Figure 5, the thoracic adhesive apparatus shows variation in the populations. According to them, *G. alidaeii* is distinguished from *G. shapuri* by having the thoracic adhesive apparatus moderately elevated (vs. strongly elevated), which is not a good taxonomic character state to distinguish these two species.

The length of barbels is another taxonomic character used by Mousavi-Sabet et al. [5] for species distinction. They mentioned that *G. alidaeii* and *G. shapuri* are distinguished from *G. silviae* by maxillary barbel as long as the head (90–110% HL); inner mandibular barbel 45–48% HL; outer mandibular barbel 67–74% HL, vs. maxillary barbel shorter than the head (76–89% HL); inner mandibular barbel 19–33% HL; and outer mandibular barbel 42–49% HL. Our data show maxillary barbel 103–117% HL (*G. silviae*); 78–121% HL (*G. alidaeii*); 88–109% HL (*G. shapuri*); 88–101% HL (*G. hosseinpanahii*) and 79–95% HL (*G. galaxias*); inner mandibular barbel 27–37% HL (*G. silviae*); 23–39% HL (*G. alidaeii*); 24–31% HL (*G. shapuri*); 26–29% HL (*G. hosseinpanahii*) and 32–37% HL (*G. galaxias*); outer mandibular barbel 54–65% HL (*G. silviae*); 42–67% HL (*G. alidaeii*); 50–59% HL (*G. shapuri*); 49–58% HL (*G. hosseinpanahii*); and 56–60% HL (*G. galaxias*). The caudal peduncle index is the other character used for distinguishing these newly described species. Our data show caudal peduncle index 1.6–2 in *G. silviae*; 1.2–1.8 in *G. alidaeii*; 1.5–1.8 in *G. shapuri*; 1.6–1.7 in *G. hosseinpanahii* and 1.2–1.6 in *G. galaxias*, which show overlap and cannot be considered as a taxonomic diagnostic character. Other characteristics, such as the thoracic

adhesive apparatus size, adipose-fin length and distance between the base of the last dorsal-fin ray and adipose-fin origin, were also used by Mousavi-Sabet et al. [5] for species distinguishing. However, we could not distinguish these newly described species based on these characters (see Table 3). Hence, due to high morphological variation (e.g., thoracic adhesive apparatus shape, barbel size, caudal peduncle index and caudal fin shape (see Figures 5 and 6 and Table 3)) among these four newly described species, we could not find a diagnostic character to distinguish and to consider them as distinct taxa.

Morphological characters can present high plasticity under environmental conditions, such as food abundance, temperature, etc. [30–33], as observed in some other taxa (e.g., the genus *Garra*).

The mental disc was used as a significant character for taxonomic and systematic inferences within the genus *Garra* [34,35]. However, in the case of the Tashan cave barb *Garra tashanensis*, inhabiting a small cave in southwest Iran, there are two forms of fishes in terms of mental discs (sucking mouth disc), including disc-bearing and disc-less fishes. However, based on most species delimitation algorithms, both forms are members of a single taxonomic unit with genetic distances of 0.3–0.8% [36]. Hence, the observed mental disc variation was not inferred to be a taxonomic character or a consequence of feature displacement. Instead, it can be considered to be a case of character release to diversify among ecological niches in the limited subterranean habitat or a case of relaxed selection, which should be clarified in detail in follow-up ecological and population genetic studies [35].

The low genetic variations between *G. alidaeii*, *G. galaxias*, *G. hosseinpanahii*, *G. shapuri* and *G. silviae* might also be explained by ecological niche variation in the closely placed river systems, the geological events, such as the Late Pleistocene glacial and recent isolation of Iranian drainage basins [37].

Based on this integrated molecular and morphological study, we treat *G. alidaeii*, *G. galaxias*, *G. hosseinpanahii* and *G. shapuri* as the junior synonyms of *G. silviae*. The species, *G. armeniacus*, *G. cous*, *G. daemon*, *G. kurdistanicus*, *G. pallens*, *G. silviae* and *G. steindachneri* are considered as valid species.

Iranian inland water habitats have been and continue to be threatened by the main causes of biodiversity loss. The taxonomic revision of the Iranian endemic group of *Glyptothorax* here has several implications for conservation: (i) it confirms the presence of two valid species in this group as the main units of conservation (i.e., *G. pallens* and *G. silviae*), (ii) it documents a narrow distributional range and diversity for *G. pallens*, but a wider distributional range and mitochondrial variability for *G. silviae* and (iii) it allows for delimiting conservation units below species level, so that limited conservation resources can be utilized optimally [38]. The molecular and morphological data indicate that *G. silviae* comprises just one evolutionary significant unit; however, according to the definition of Moritz [39], this evolutionary unit is best viewed as comprising five management units corresponding to each of the identified subclades. *Glyptothorax silviae* has a high level of genetic diversity if treated as only one panmictic group; however, species structured into management units necessitate separate monitoring and management of each unit [40,41].

Supplementary Materials: The following supporting information can be downloaded at: https://www.mdpi.com/article/10.3390/d14100884/s1, Tables S1: Primers used to amplify and their sequences; Table S2: List of different *Glyptothorax* species from outside the Middle East used in this study; Table S3: GenBank accession numbers (seq. ID/GenBank number) for the new *Glyptothorax* material examined from the Middle East (details of the specimens are given in Table 1); Table S4: Results of the Xia's nucleotide substitution saturation test for COI, *Cyt* b and RAG2 of the studied *Glyptothorax* specimens.

Author Contributions: Conceptualization, G.S., F.Z. and H.R.E.; methodology, G.S., F.Z. and H.R.E.; formal analysis, G.S., F.Z. and H.R.E.; investigation, G.S., F.Z. and H.R.E.; resources, H.R.E.; writing—original draft preparation, G.S., F.Z. and H.R.E.; writing—review and editing, G.S., F.Z. and H.R.E.; supervision, H.R.E.; project administration, H.R.E.; funding acquisition, H.R.E. All authors have read and agreed to the published version of the manuscript.

Funding: The research work was funded by Shiraz University (SU-9233856).

Institutional Review Board Statement: Not applicable.

Informed Consent Statement: Not applicable.

Data Availability Statement: The new DNA sequences (COI: OP585111–OP585139; *Cyt* b: OP589359–OP589381; RAG2: OP589382–OP589398) and voucher specimens used in this study are deposited in GenBank and ZM-CBSU, respectively.

Acknowledgments: We are pleased to thank Marie-Hélène Hubert and Kamal Khidas (CMNFI) for sending pictures of the types of *G. silviae*, James McLane (BMNH) for providing pictures of the type of *G. cous* and Farahani for DNA extraction of some specimens.

Conflicts of Interest: The authors declare no conflict of interest.

References

1. Fricke, R.; Eschmeyer, W.N.; Van der Laan, R. Eschmeyer's Catalog of Fishes: Genera, Species, References. Available online: http://researcharchive.calacademy.org/research/ichthyology/catalog/fishcatmain.asp (accessed on 15 May 2022).
2. Ferraris, C.J. Checklist of catfishes, recent and fossil (Osteichthyes: Siluriformes), and catalogue of siluriform primary types. *Zootaxa* **2007**, *1418*, 1–628. [CrossRef]
3. Ng, H.H.; Kottelat, M. The identity of *Clarias batrachus* (Linnaeus, 1758), with the designation of a neotype (Teleostei: Clariidae). *Zool. J. Linn. Soc.* **2008**, *153*, 725–732. [CrossRef]
4. Freyhof, J.; Kaya, C.; Abdullah, Y.S.; Geiger, M.F. The *Glyptothorax* catfishes of the Euphrates and Tigris with the description of a new species (Teleostei: Sisoridae). *Zootaxa* **2021**, *4969*, 453–491. [CrossRef]
5. Mousavi-Sabet, H.; Eagderi, S.; Vatandoust, S.; Freyhof, J. Five new species of the sisorid catfish genus *Glyptothorax* from Iran (Teleostei: Sisoridae). *Zootaxa* **2021**, *5067*, 451–484. [CrossRef] [PubMed]
6. Ng, H.H.; Dodson, J.J. Morphological and genetic descriptions of a new species of catfish, *Hemibagrus chrysops*, from Sarawak, east Malayasia, with an assessment of phylogenetic relationships (Teleostei: Bagridae). *Raffles Bull. Zool.* **1999**, *47*, 45–47.
7. Bruford, M.W.; Hanotte, O.; Brookfield, J.F.Y.; Burke, T.A. Single-locus and multilocus DNA fingerprinting. In *Molecular Genetics Analysis of Populations: A Practical Approach*; Hoezel, C., Ed.; Oxford University Press: Oxford, UK, 1992; pp. 225–269.
8. Jiang, W.; Ng, H.H.; Yang, J.; Chen, X. Monophyly and phylogenetic relationships of the catfish genus *Glyptothorax* (Teleostei: Sisoridae) inferred from nuclear and mitochondrial gene sequences. *Mol. Phylogenet. Evol.* **2011**, *61*, 278–289. [CrossRef]
9. Zarei, F.; Esmaeili, H.R.; Schliewen, U.K.; Abbasi, K.; Sayyadzadeh, G. Mitochondrial phylogeny, diversity, and ichthyogeography of gobies (Teleostei: Gobiidae) from the oldest and deepest Caspian sub-basin and tracing source and spread pattern of an introduced *Rhinogobius* species at the tricontinental crossroad. *Hydrobiologia* **2021**, *848*, 1267–1293. [CrossRef]
10. Sullivan, J.P.; Lundberg, J.G.; Hardman, M. A phylogenetic analysis of the major groups of catfishes (Teleostei: Siluriformes) using RAG1 and RAG2 nuclear gene sequences. *Mol. Phylogenet. Evol.* **2006**, *41*, 636–662. [CrossRef]
11. Chen, W.; Ma, X.; Shen, Y.; Mao, Y.; He, S. The fish diversity in the upper reaches of the Salween River, Nujiang River, revealed by DNA barcoding. *Sci. Rep.* **2015**, *5*, 17437. [CrossRef]
12. Peng, Z.; Ho, S.Y.; Zhang, Y.; He, S. Uplift of the Tibetan plateau: Evidence from divergence times of glyptosternoid catfishes. *Mol. Phylogenet. Evol.* **2006**, *39*, 568–572. [CrossRef]
13. Hall, T. BioEdit: A user-friendly biological sequence alignment editor and analysis program for windows 95/98/NT. *Nucleic Acids Symp. Ser.* **1999**, *41*, 95–98.
14. Kumar, S.; Stecher, G.; Tamura, K. MEGA7: Molecular evolutionary genetics analysis version 7.0 for bigger datasets. *Mol. Biol. Evol.* **2016**, *33*, 1870–1874. [CrossRef] [PubMed]
15. Akaike, H. A new look at the statistical model identification. *IEEE Trans. Automat. Contr.* **1974**, *19*, 716–723. [CrossRef]
16. Darriba, D.; Taboada, G.L.; Doallo, R.; Posada, D. jModelTest 2: More models, new heuristics and parallel computing. *Nat. Methods* **2012**, *9*, 772. [CrossRef] [PubMed]
17. Xia, X.; Xie, Z.; Salemi, M.; Chen, L.; Wang, Y. An index of substitution saturation and its application. *Mol. Phylogenet. Evol.* **2003**, *26*, 1–7. [CrossRef]
18. Xia, X. DAMBE7: New and improved tools for data analysis in molecular biology and evolution. *Mol. Biol. Evol.* **2018**, *35*, 1550–1552. [CrossRef]
19. Ronquist, F.; Teslenko, M.; Van Der Mark, P.; Ayres, D.L.; Darling, A.; Höhna, S.; Larget, B.; Liu, L.; Suchard, M.A.; Huelsenbeck, J.P. MrBayes 3.2: Efficient Bayesian phylogenetic inference and model choice across a large model space. *Syst. Biol.* **2012**, *61*, 539–542. [CrossRef]
20. Stamatakis, A. RAxML-VI-HPC: Maximum likelihood-based phylogenetic analyses with thousands of taxa and mixed models. *Bioinformatics* **2006**, *22*, 2688–2690. [CrossRef]
21. Felsenstein, J. Confidence limits on phylogenies: An approach using the bootstrap. *Evolution* **1985**, *39*, 783–791. [CrossRef]
22. Puillandre, N.; Lambert, A.; Brouillet, S.; Achaz, G. ABGD, Automatic Barcode Gap Discovery for primary species delimitation. *Mol. Ecol.* **2012**, *21*, 1864–1877. [CrossRef]

23. Puillandre, N.; Brouillet, S.; Achaz, G. ASAP: Assemble species by automatic partitioning. *Mol. Ecol. Resour.* **2021**, *21*, 609–620. [CrossRef] [PubMed]
24. Hart, M.W.; Sunday, J. Things fall apart: Biological species form unconnected parsimony networks. *Biol. Lett.* **2007**, *3*, 509–512. [CrossRef] [PubMed]
25. Kapli, P.; Lutteropp, S.; Zhang, J.; Kobert, K.; Pavlidis, P.; Stamatakis, A.; Flouri, T. Multi-rate Poisson tree processes for single-locus species delimitation under maximum likelihood and Markov Chain Monte Carlo. *Bioinformatics* **2017**, *33*, 1630–1638. [CrossRef] [PubMed]
26. Clement, M.; Posada, D.; Crandall, K.A. TCS: A computer program to estimate gene genealogies. *Mol. Ecol.* **2000**, *9*, 1657–1659. [CrossRef] [PubMed]
27. Leigh, J.W.; Bryant, D. Popart: Full-feature software for haplotype network construction. *Methods Ecol. Evol.* **2015**, *6*, 1110–1116. [CrossRef]
28. Ward, R.D. DNA barcode divergence among species and genera of birds and fishes. *Mol. Ecol. Resour.* **2009**, *9*, 1077–1085. [CrossRef]
29. Yeates, D.K.; Seago, A.; Nelson, L.; Cameron, S.L.; Joseph, L.; Trueman, J.W. Integrative taxonomy, or iterative taxonomy? *Syst. Entomol.* **2011**, *36*, 209–217. [CrossRef]
30. Allendorf, F.W.; Phelps, S.R. Loss of genetic variation in hatchery stock of cutthroat trout. *Trans. Am. Fish. Soc.* **1988**, *109*, 537–543. [CrossRef]
31. Swain, D.P.; Foote, C.J. Stocks and chameleons: The use of phenotypic variation in stock identification. *Fish. Res.* **1999**, *43*, 113–128. [CrossRef]
32. Wimberger, P.H. Plasticity of fish body shape, the effects of diet, development, family and age in two species of *Geophagus* (Pisces: Cichlidae). *Biol. J. Linn. Soc.* **1992**, *45*, 197–218. [CrossRef]
33. Turan, C.; Oral, M.; Ozturk, B.; Duzgunes, E. Morphometric and meristic variation between stocks of bluefish (*Pomatomus saltatrix*) in the Black, Marmara, Aegean and northeastern Mediterranean Seas. *Fish. Res.* **2005**, *79*, 139–147. [CrossRef]
34. Hashemzadeh Segherloo, I.; Bernatchez, L.; Golzarianpour, K.; Abdoli, A.; Primmer, C.R.; Bakhtiary, M. Genetic differentiation between two sympatric morphs of the blind Iran cave barb *Iranocypris typhlops*. *J. Fish Biol.* **2012**, *81*, 1747–1753. [CrossRef] [PubMed]
35. Hashemzadeh Segherloo, I.; Normandeau, E.; Benestan, L.; Rougeux, C.; Coté, G.; Moore, J.S.; Ghaedrahmati, N.; Abdoli, A.; Bernatchez, L. Genetic and morphological support for possible sympatric origin of fish from subterranean habitats. *Sci. Rep.* **2018**, *8*, 2909. [CrossRef] [PubMed]
36. Hashemzadeh Segherloo, I.; Najafi Chaloshtory, S.; Naser, M.D.; Yasser, A.G.; Tabatabaei, S.N.; Piette-Lauziere, G.; Mashtizadeh, A.; Elmi, A.; Sedighi, O.; Changizi, A.; et al. Sympatric morphotypes of the restricted-range Tashan Cave *Garra*: Distinct species or a case of phenotypic plasticity? *Environ. Biol. Fishes* **2022**, *105*, 1251–1260. [CrossRef]
37. Esmaeili, H.R.; Teimori, A.; Sayyadzadeh, G.; Masoudi, M.; Reichenbacher, B. Phylogenetic relationships of the tooth-carp *Aphanius* (Teleostei: Cyprinodontidae) in the river systems of southern and south-western Iran based on mtDNA sequences. *Zool. Middle East* **2014**, *60*, 29–38. [CrossRef]
38. Ryder, O.A. Species conservation and systematics: The dilemma of subspecies. *Trends Ecol. Evol.* **1986**, *1*, 9–10. [CrossRef]
39. Moritz, C. Defining "evolutionarily significant units" for conservation. *Trends Ecol. Evol.* **1994**, *9*, 373–375. [CrossRef]
40. Frankham, R.; Ballou, J.D.; Briscoe, D.A. *Introduction to Conservation Genetics*; Cambridge University Press: Cambridge, UK, 2002.
41. Zarei, F.; Esmaeili, H.R.; Sadeghi, R.; Schliewen, U.K.; Kovačić, M.; Abbasi, K.; Gholamhosseini, A. An integrative insight into the diversity, distribution and biogeography of the freshwater endemic clade of the *Ponticola syrman group* (Teleostei: Gobiidae). *Ecol. Evol.* **2022**, *12*, e9300. [CrossRef]